From the Archives of the AFIP

Neoplasms of the Spinal Cord and Filum Terminale: Radiologic-Pathologic Correlation[1]

CME FEATURE

See accompanying test at http://www.rsna.org/education/rg_cme.html

LEARNING OBJECTIVES FOR TEST 6

After reading this article and taking the test, the reader will be able to:

- List the essential imaging features of intramedullary spinal cord neoplasms.
- Identify the characteristic imaging appearances of the different types of intramedullary spinal cord neoplasms that allow a specific diagnosis to be favored.
- Describe the correlation of the imaging appearance with the gross pathologic appearance in intramedullary spinal neoplasms.

Kelly K. Koeller, CDR, MC, USN • R. Scott Rosenblum, DO • Alan L. Morrison, CDR, MC, USN

Intramedullary spinal cord neoplasms are rare, accounting for about 4%–10% of all central nervous system tumors. Despite their rarity, these lesions are important to the radiologist because magnetic resonance (MR) imaging is the preoperative study of choice to narrow the differential diagnosis and guide surgical resection. On contrast material–enhanced MR images, intramedullary spinal tumors almost always manifest as expansion of the spinal cord and show enhancement. Syringohydromyelia and cystic lesions are frequently associated with intramedullary tumors. Nontumoral cysts tend to be located at the poles of the tumors and do not enhance on contrast-enhanced MR images, whereas cysts within the substance of the tumor are considered tumoral cysts and typically demonstrate peripheral enhancement. Spinal cord ependymomas are the most common type in adults, and cord astrocytomas are most common in children. Both entities constitute up to 70% of all intramedullary neoplasms. A central location within the spinal cord, presence of a cleavage plane, and intense homogeneous enhancement are imaging features that favor an ependymoma. Intramedullary astrocytomas are usually eccentrically located within the cord, are ill defined, and have patchy enhancement after intravenous contrast material administration. Even with these characteristics, it may not be possible to differentiate these two entities on the basis of imaging features alone. Cord hemangioblastomas are the third most common type of intramedullary spinal tumor. Gangliogliomas commonly extend over more than eight vertebral segments. Paragangliomas and primitive neuroectodermal tumors have an affinity for the filum terminale and cauda equina. Other spinal cord tumors include metastatic disease, which is characterized by prominent cord edema for the size of the enhancing portion, and primary lymphoma.

Abbreviations: CNS = central nervous system, H-E = hematoxylin-eosin, PNET = primitive neuroectodermal tumor, WHO = World Health Organization

Index terms: Spinal cord, MR, 30.1214 • Spinal cord, neoplasms, 30.32, 30.33, 30.363 • Spinal cord, US, 30.1298

RadioGraphics 2000; 20:1721–1749

[1]From the Departments of Radiologic Pathology (K.K.K., R.S.R.) and Neuropathology (A.L.M.), Armed Forces Institute of Pathology, 14th St at Alaska Ave, Bldg 54, Rm M-121, Washington, DC 20306-6000; and the Departments of Radiology and Nuclear Medicine (K.K.K.) and Pathology (A.L.M.), Uniformed Services University of the Health Sciences, Bethesda, Md. Received May 11, 2000; revision requested May 30; revision received July 12; accepted July 18. **Address correspondence to** K.K.K. (e-mail: *koeller@afip.osd.mil*).

Introduction

Spinal intramedullary neoplasms account for about 4%–10% of all central nervous system (CNS) tumors and about 2%–4% of CNS glial tumors. Although spinal cord neoplasms constitute only 20% of all intraspinal tumors in the adult population, they constitute 35% of such tumors in children (1). Most spinal cord neoplasms are malignant, and 90%–95% are classified as gliomas. Most of these glial neoplasms are either ependymomas or astrocytomas. Ependymomas are the most common glial tumor in adults, whereas astrocytomas are the most common intramedullary tumor in children. Nonglial neoplasms, including hemangioblastomas, paragangliomas, metastases, lymphoma, and primitive neuroectodermal tumors (PNETs), are much less common (Table 1). In contrast to intracranial neoplasms, the vast majority of spinal cord neoplasms, including even low-grade forms, enhance after the administration of contrast material to at least some degree. Enhanced areas probably represent more active portions of the tumors and may indicate potential sites for biopsy if resection is not feasible.

In this article, we correlate the imaging features of intramedullary spinal neoplasms with the underlying pathologic findings by using cases from the Thompson Archives of the Department of Radiologic Pathology at the Armed Forces Institute of Pathology, Washington, DC. After reviewing the use of magnetic resonance (MR) imaging in the evaluation of spinal cord neoplasms, we describe and illustrate the prevalence and clinical, pathologic, and imaging characteristics of ependymoma and its variants, astrocytoma, ganglioglioma, hemangioblastoma, paraganglioma, metastasis, lymphoma, and PNETs.

Table 1
Neoplasms of the Spinal Cord and Filum Terminale

Common
Ependymoma
Myxopapillary ependymoma
Astrocytoma
Pilocytic astrocytoma
Anaplastic astrocytoma
Hemangioblastoma
Less common
Subependymoma
Ganglioglioma
Paraganglioma
Metastasis
Lymphoma
PNET
Neurocytoma
Oligodendroglioma
Mixed glioma
Glioblastoma multiforme

Overview of Intramedullary Spinal Neoplasms

Traditional imaging modalities (conventional radiography and computed tomography [CT]) of the mid-20th century often failed to reveal the true extent of intramedullary spinal neoplasms until gross expansion of the spinal canal had occurred. Myelography, either with conventional radiography or CT, revealed an intramedullary mass as a complete or partial block in the flow of intrathecal contrast material (Fig 1). Myelography, however, could rarely help define the character of the spinal cord lesion. The development of magnetic resonance (MR) imaging revolutionized the noninvasive investigation of these lesions. Identification of internal structural abnormalities of the spinal cord, such as cysts, syringohydromyelia, hemorrhage, and edema, became routine in the setting of an intramedullary spinal mass. Not surprisingly, MR imaging is the current imaging modality of choice in the evaluation of spinal cord masses.

The "basic" spinal MR imaging study should include unenhanced T1- and T2-weighted images in the sagittal plane and contrast material–enhanced T1-weighted images in the sagittal and axial planes. Contrast-enhanced images are especially valuable for determining the solid portion of an intramedullary neoplasm and identifying associated cysts and other features that often modify the differential diagnosis (2). Advances in the development of imaging software and improved surface coil technology have facilitated

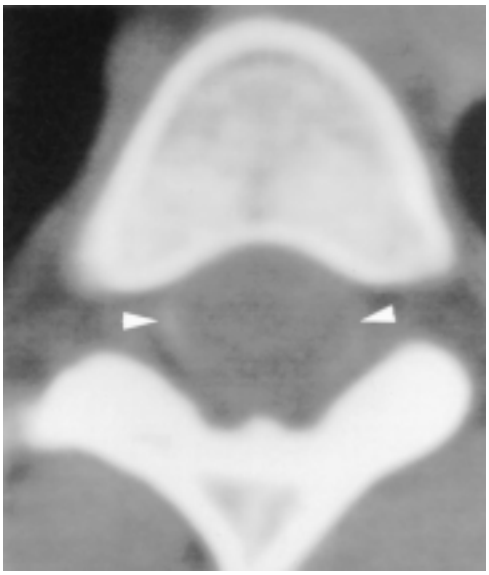

Figure 1. Intramedullary astrocytoma in an 18-year-old woman with progressive paresis, paresthesia of the lower extremities, and difficulty voiding. CT myelogram shows a near-compete block of intrathecal contrast material (arrowheads) secondary to an intramedullary mass. No additional information can be discerned from the spinal cord lesion, which reflects a substantial shortcoming of this imaging modality.

the imaging of a patient suspected of having intramedullary disease. Phased-array surface coils, in particular, save valuable time because they allow basion-to-conus evaluation of the spinal cord in a single sequence (3). In addition, postoperative assessment is best performed with a contrast-enhanced MR imaging examination, which has become the sine qua non for establishing the presence of recurrent tumor (4–7). Still, although MR imaging is a powerful tool, it is not perfect. In a series of 171 patients with spinal cord tumors (8), MR imaging findings could correctly suggest the histologic diagnosis in only 70% of cases. In particular, the differentiation of ependymoma from astrocytoma was the most difficult with MR imaging alone.

There are three important tenets in the use of MR imaging to evaluate patients suspected of having an intramedullary spinal process. First, the essential imaging criterion for an intramedullary spinal neoplasm is cord expansion (9). If this feature is absent, it should suggest a nonneoplastic etiology, such as demyelinating disease, sarcoidosis, amyloid angiopathy, pseudotumor, dural arteriovenous fistula, cord infarction, chronic arachnoiditis, or cystic myelomalacia (10–12). Obviously, the differentiation of neoplastic from nonneoplastic entities is crucial to the surgeon. If a lesion is likely to be a neoplasm, the patient may be a candidate for a gross total resection of the mass after the tumor is debulked. If the lesion is not likely to be a tumor, only a biopsy is initially indicated. Once the nonneoplastic cause is confirmed, appropriate (and usually nonsurgical) therapy can be instituted. Accordingly, patients with nonsurgical disease can be spared the risks of an aggressive surgical approach with much less postoperative morbidity (10). In a series of 212 patients suspected of having intramedullary disease (10), nine (4%) had nonneoplastic lesions. None of the nine patients had imaging evidence of cord expansion.

Second, the vast majority of intramedullary spinal neoplasms show at least some enhancement following the intravenous administration of gadolinium-based contrast material (6,12–15). Accordingly, in the evaluation of a patient suspected of harboring such a lesion, obtaining contrast-enhanced images in at least two different planes is essential, not only for limiting the differential diagnosis but also for planning surgery. However, although almost all spinal cord tumors show some enhancement, the converse is not true: The absence of enhancement does not exclude an intramedullary neoplasm in the presence of cord expansion (16).

Third, cysts are a common associated finding in the setting of an intramedullary spinal tumor. There are two basic types of cysts: tumoral and nontumoral. Cysts located at the poles of the solid portion of the tumor usually represent simply reactive dilatation of the central canal (syringomyelia). Approximately 60% of all intramedullary spinal tumors demonstrate these rostral or caudal

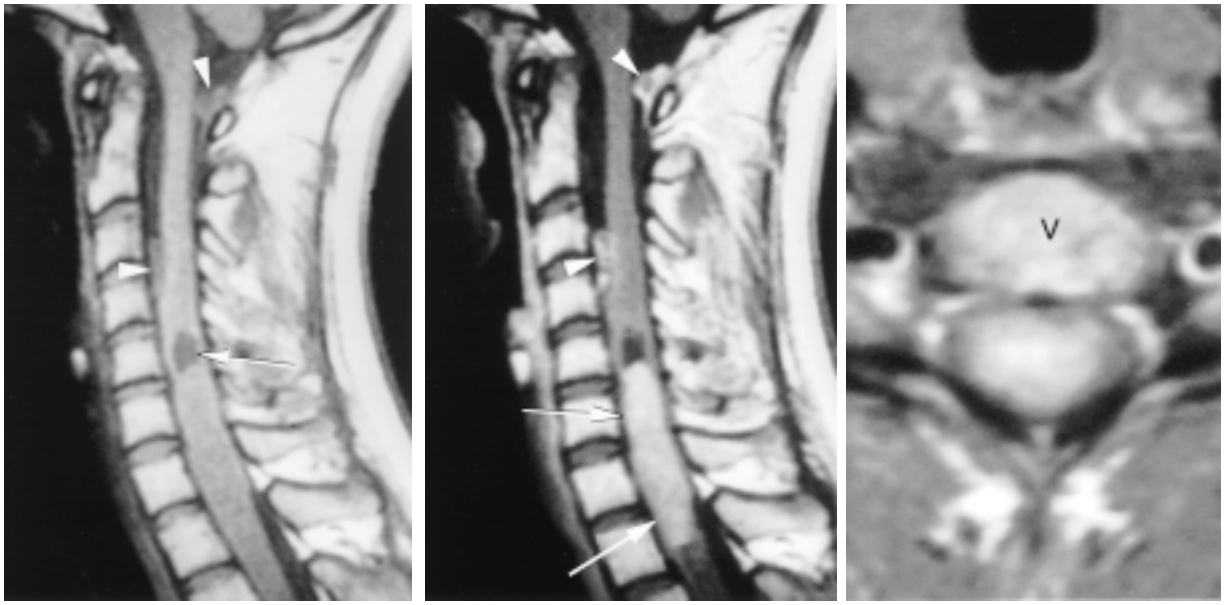

a. **b.** **c.**

Figure 2. Ependymoma and meningiomas in a 27-year-old woman with neck pain. **(a)** Sagittal T1-weighted MR image shows lower cervical cord expansion. Except for a cystlike area of low signal intensity (arrow), the mass is nearly isointense relative to the normal spinal cord. There are separate intradural, extramedullary masses (arrowheads) of the intradural compartment at C1 and C3-4. **(b)** Contrast-enhanced sagittal T1-weighted MR image demonstrates homogeneous enhancement of the oval mass (arrows) extending from C5-6 to T1. The extramedullary lesions (arrowheads) also enhance intensely. **(c)** Contrast-enhanced axial T1-weighted MR image shows intense enhancement within the cervical spinal cord. Results of histologic examination confirmed that the intramedullary mass was an ependymoma and the extramedullary lesions were meningiomas. *v* = vertebral body.

(also called polar or satellite) cysts (Fig 2). In these cases, only the solid component of a spinal cord tumor must be resected; the rostral and caudal cysts will either decompress upon removal of the solid portion or they can be aspirated by the surgeon at resection (17). These cysts are not part of the tumor itself and should not enhance on imaging studies. They are not septated and do not show echogenicity within their walls at intraoperative ultrasonography (US) (17). Polar cysts are believed to arise from the egress of fluid produced by these neoplasms through the central canal and may also explain the relative lack of symptoms seen in cases of intramedullary spinal neoplasms (18). In contrast, tumoral cysts are contained within the tumor itself and frequently show peripheral enhancement (Fig 3) (16). They tend to be more commonly seen in astrocytomas than in ependymomas (17). Identification of the location of the solid enhancing portion of the tumor (including enhancing tumoral cysts) is vital because current neurosurgical techniques allow laminotomy or laminectomy to be limited only to this zone, thereby decreasing potential surgical morbidity. Finally, intraoperative monitoring of somatosensory-evoked potentials and use of the Cavitron ultrasonic surgical aspirator (Cusa Valleylab, Boulder, Colo) have greatly facilitated the surgical resection of many intramedullary neoplasms (8,19).

Some clinical associations with intramedullary spinal cord tumors are noteworthy. Intramedullary spinal neoplasms are more common in patients with neurofibromatosis, with ependymomas occurring more often in patients with type 2 disease and with astrocytomas occurring more frequently in those with type 1 disease. It is speculated that the same molecular mechanisms

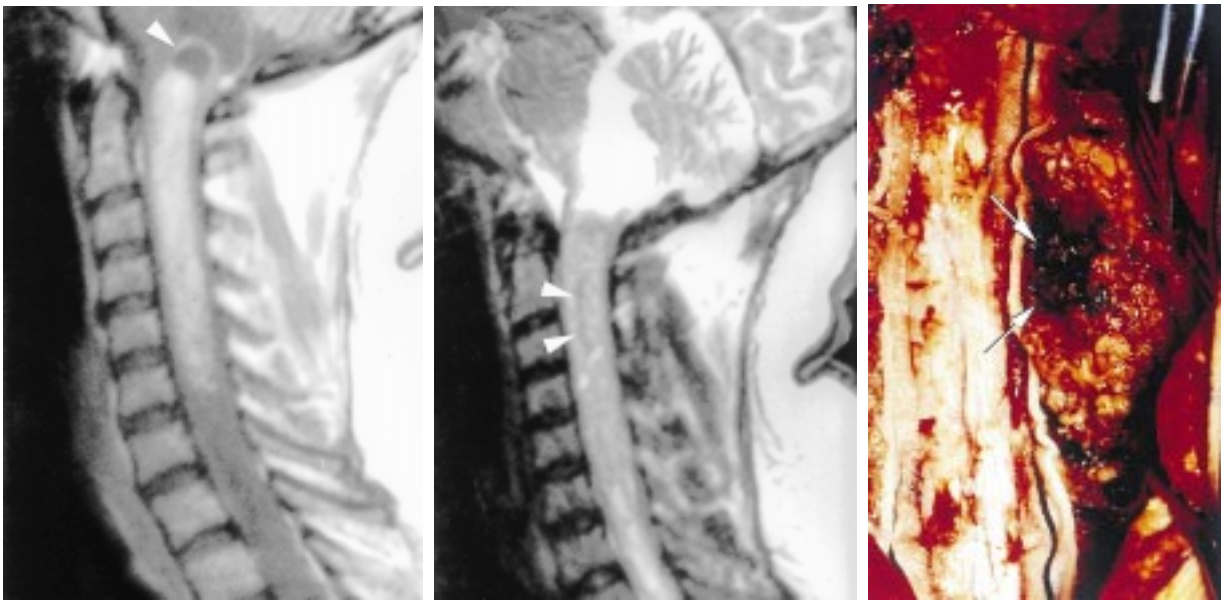

a. b. c.

Figure 3. Ependymoma in a 32-year-old woman with upper- and lower-extremity weakness and numbness and bowel and bladder dysfunction. **(a)** Contrast-enhanced sagittal T1-weighted MR image demonstrates a heterogeneously enhancing mass expanding the cervical spinal cord. A cyst with faint peripheral enhancement (arrowhead) is seen at the superior pole of the mass. **(b)** Sagittal T2-weighted MR image reveals that the mass is predominantly isointense relative to the spinal cord, with scattered areas of high signal intensity. There is a curvilinear area of low signal intensity (arrowheads) at the C2-3 level, which is suggestive of hemorrhage. **(c)** Intraoperative photograph demonstrates the lobulated, irregular mass with areas of hemorrhage (arrows).

responsible for the increased prevalence of intracranial tumors in patients with neurofibromatosis also cause the increased rate for intraspinal tumors (20). The biologic behaviors of neoplasms of the cervicomedullary junction are more like those of spinal cord tumors (more benign) than those of brainstem gliomas (more aggressive) (21,22). Finally, the higher the location of an intramedullary spinal tumor, the more likely that a syrinx will develop (23).

Glial Neoplasms

Ependymoma

Prevalence.—Ependymoma is the most common intramedullary spinal neoplasm in adults, accounting for up to 60% of all glial spinal cord tumors (19). From the four largest studies of patients with spinal cord ependymomas reported in the literature (5,19,24,25), the following demographic information emerges: These lesions tend to manifest in young adulthood, with a mean age at presentation of 38.8 years and are more common in male patients (57.4%). Cord ependymomas occur most commonly in the cervical region, with 44% involving the cervical cord alone and an additional 23% extending into the upper thoracic region. About 26% are located in the thoracic cord alone. Only 6.5% involve either the distal thoracic cord or the conus medullaris (5,19,24, 25). Myxopapillary ependymoma, a variant type, is, in rare cases, found in the subcutaneous tissue of the sacrococcygeal region, usually without any connection with the spinal canal (26). It is believed that these arise from either heterotopic ependymal cell rests or vestigial remnants of the distal neural tube during canalization and retrogressive differentiation (26,27).

Clinical Presentation.—As with most primary intramedullary tumors, there is frequently a long antecedent history before the diagnosis of an intramedullary ependymoma is established. The mean duration of symptoms was 36.5 months for the 183 patients from the four largest studies (5, 19,24,25). A large majority of patients with spinal cord ependymomas have relatively mild clinical symptoms. Most of the 183 patients (81%) could walk without assistance at presentation (5,24,25). In general, the less preoperative neurologic deficit existing at presentation, the better the postoperative outcome (5,25). Typically, patients initially present with mild symptoms, and there is no objective evidence of neurologic deficits, which often leads to a delay in diagnosis (5,19,24,25). Some ependymomas may even be a source of subarachnoid hemorrhage (28,29).

At diagnosis, patients with spinal cord ependymomas typically have back or neck pain (67%), sensory deficits (52%), motor weakness (46%), or bowel or bladder dysfunction (15%) (5,19,24, 25). The predominance of sensory symptoms (85% of patients with pain and other sensory deficits combined) may be directly related to the more central location of these tumors (5). Spinal cord ependymomas are believed to arise from ependymal cells that line the central canal. Theoretically, this central location makes it likely that the crossing spinothalamic tracts will be compressed or interrupted. Dominant motor symptoms are commonly associated with very large ependymomas and a poorer postoperative outcome secondary to the increased surgical risk associated with resection of these larger lesions (5). Hoshimaru et al (25) found that patients with a shorter duration of symptoms tended to have a better postoperative outcome. Lesions of the thoracic cord are associated with poorer surgical outcomes, perhaps because of its relatively tenuous vascular supply, compared with lesions of the cervical spinal cord. This was especially true in patients with evidence of arachnoid scarring or cord atrophy at surgery (25).

Intramedullary ependymomas are characterized by slow growth and tend to compress adjacent spinal cord tissue rather than infiltrate it. Accordingly, there is almost always a cleavage plane, which facilitates microsurgical resection, the treatment of choice (5,19,24,25). Patients frequently have worsened symptoms in the immediate postoperative period secondary to edema and possibly transient interference with spinal cord blood flow (5,25,30). Postoperative radiation therapy is reserved for recurrent disease, which is much more commonly seen in cases of subtotal resection (5,25,30). The patient's preoperative neurologic status is the most important predictor of outcome (5,19,24). Earlier surgical resection is associated with fewer and less severe neurologic deficits. Recurrence is substantially reduced when a complete gross total resection can be performed (5,19,30). The 5-year survival rate for patients with spinal cord ependymomas is approximately 82%, regardless of how severe the preoperative neurologic deficits. The 20-year survival rate, however, is much worse for patients who present with a major neurologic dysfunction (50%) than for patients with a minor neurologic impairment (33%) (19). The lungs, retroperitoneum, and lymph nodes are the most common extraspinal sites of metastatic spread (31).

Pathologic Characteristics.—Most ependymomas displace rather then infiltrate adjacent neural tissue. Because ependymomas are believed to arise from ependymal cells of the central canal within the spinal cord, symmetric cord expansion is the rule. These soft, friable, well-marginated lesions are frequently gray and have associated syringomyelia (32). Polar cysts are a common finding (62% in the study by Brotchi and Fischer [24]). True tumoral cysts are less common (22% of cases) (24). Small feeding vessels at the ventral surface are commonly noted at surgical resection (5,25). The myxopapillary variant is virtually always located along the filum terminale with occasional extension to the conus medullaris and may appear as a soft, tannish "bag" of tissue (32).

Uniform, moderately hyperchromatic nuclei are typical findings at histologic examination (Fig 4) (32). Six histologic types are recognized: cellular

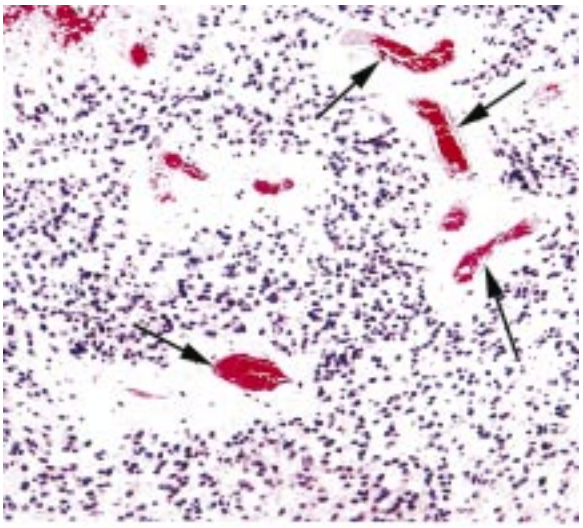

Figure 4. Photomicrograph (original magnification, ×100; hematoxylin-eosin [H-E] stain) of a spinal cord ependymoma shows ependymal cells with uniform hyperchromatic nuclei arranged in perivascular pseudorosettes (arrows).

(the classic and most common type), papillary, clear cell, tanycytic, myxopapillary, and melanotic (the least common type) (32). Perivascular pseudorosettes are virtually required to establish the diagnosis of ependymoma but may be less conspicuous in less cellular types of ependymomas. With use of the World Health Organization (WHO) classification (24), almost all spinal cord ependymomas can be classified as either grade I or grade II. Malignant types are rare (32). Cystic degeneration is seen in 50% of cases, and hemorrhage is common (especially at the superior and inferior margins of the tumor). In contrast to intracranial ependymomas, calcification is uncommon.

Rarely, a cord ependymoma may extend exophytically and present a diagnostic challenge (8). Ependymomas may even arise outside the CNS (sacrococcygeal region, broad ligament of the ovary). Up to one-third of these ectopically located ependymomas are associated with spina bifida occulta (33).

Results of recent investigations reveal mutations of the type 2 neurofibromatosis transcript in some cases of sporadic spinal cord ependymomas that occurred in patients without type 2 neurofibromatosis. These changes have not been observed in intracranial ependymomas and, therefore, are suggestive of a different molecular basis for ependymomas that arise in the spinal cord (34).

Imaging Characteristics.—Radiographs of patients with ependymomas may reveal scoliosis (16% of cases) or canal widening (11%) with associated vertebral body scalloping, pedicle erosion, or laminar thinning (19). Conventional myelography frequently reveals either a complete or partial block in the flow of contrast material (19). At unenhanced CT, ependymomas are either isoattenuated or slight hyperattenuated compared with the normal spinal cord (19). Ependymomas enhance intensely after intravenous administration of iodinated contrast material. CT myelography shows nonspecific cord enlargement (19).

Most spinal cord ependymomas are iso- or hypointense relative to the spinal cord on T1-weighted MR images (24,35,36). In rare cases, they may manifest as a hyperintense mass, usually secondary to the effects of hemorrhage (24, 35,36). On T2-weighted images, the lesions are typically hyperintense relative to the spinal cord (35,36), although in the single largest review of spinal ependymomas, isointense tumors were as common as hyperintense tumors (24). About 20%–33% of ependymomas demonstrated the "cap sign," a rim of extreme hypointensity (hemosiderin) seen at the poles of the tumor on T2-weighted images. This finding is thought to be secondary to hemorrhage, which is common in ependymomas and other highly vascular tumors (eg, paraganglioma, hemangioblastoma) (16,35). Most cases (60%) also showed evidence of cord edema around the masses (24). The average number of vertebral segments involved with abnormal signal intensity is 3.6; however, some ependymomas may involve as many as 15 segments (19,24,25,35,36). Despite the theoretic

support for cord ependymomas having a central location on the basis of the presence of ependymal cells in the central canal, only 62.5%–76% of these tumors have been reported to arise from a central location (16,35).

Cysts are a common feature, with 78%–84% of ependymomas having at least one cyst (Figs 2, 3), most of which are the nontumoral (polar) variety (24,35,36). The prevalence of tumoral cysts appears to be more variable (4%–50% of cases) (24,35,36). Syringohydromyelia is also quite variable in previously published reports, occurring in 9%–50% of cases (Fig 5) (24,36). Analysis in one published case revealed that the syringomyelia fluid had a protein content consistent with that of an exudate, which supports the hypothesis that the cavity resulted from a disruption of the blood-brain barrier (37). When the data from the three largest studies evaluating contrast enhancement on MR images are combined, the vast majority of spinal cord ependymomas (84%) enhanced to at least some degree following the intravenous administration of gadolinium-based contrast material and even more (89%) had well-defined margins on the contrast-enhanced images (Figs 2, 3) (5,24,36).

Intraoperative US reveals ependymomas as regions of sharply defined uniform echogenicity. Cysts are easily seen with this modality (5).

Myxopapillary Ependymoma

A special variant of ependymoma, the myxopapillary ependymoma constitutes about 13% of all spinal ependymomas (38). This tumor tends to have an earlier clinical presentation (mean age, 35 years) and is more commonly seen in male patients. These mucoid tumors have a distinct predilection for the conus medullaris or filum terminale and are thought to arise from the ependymal glia of the filum terminale. Consequently, myxopapillary ependymomas are the most common neoplasm (83% of cases) in this region (38). Occasionally, they occur in the extradural space, probably arising from the coccygeal medullary vestige at the distal portion of the neural tube (39). Multiple lesions have been variably reported in about 14%–43% of cases (39).

Myxopapillary ependymomas usually manifest with lower back, leg, or sacral pain and weakness

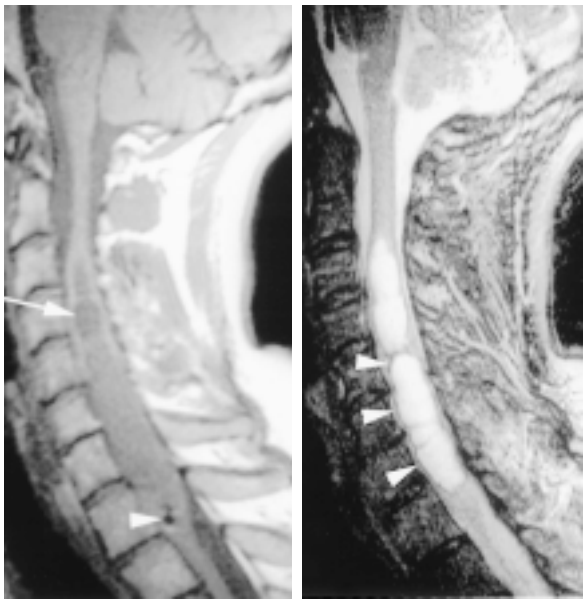

a. **b.**

Figure 5. Intramedullary ependymoma in a 42-year-old man with a 3-month history of neck pain and upper-extremity numbness. **(a)** Sagittal T1-weighted MR image shows an expanded spinal cord from C2 through T2, with associated septated syringohydromyelia (arrow). The expanded cord is slightly hyperintense relative to cerebrospinal fluid. There is a focal area of low signal intensity (arrowhead) at the caudal pole of the tumor, which is suggestive of calcification or hemosiderin deposition. **(b)** Sagittal T2-weighted MR image reveals a septated syringohydromyelia. The inner surface of the cyst has low signal intensity (arrowheads), which is consistent with prior hemorrhage. The mass fragmented into multiple irregular, nodular, reddish-brown masses at surgical resection. Results of histologic examination revealed ependymoma.

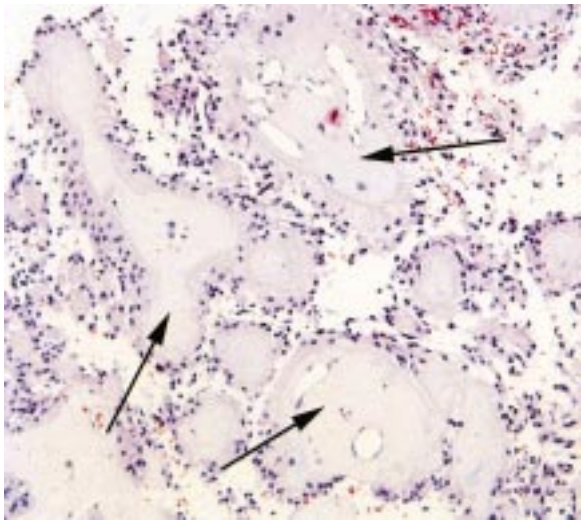

Figure 6. Photomicrograph (original magnification, ×100; H-E stain) of a myxopapillary ependymoma reveals fibrovascular cores and mucoid material (arrows) in papillary formations lined with ependymal cells.

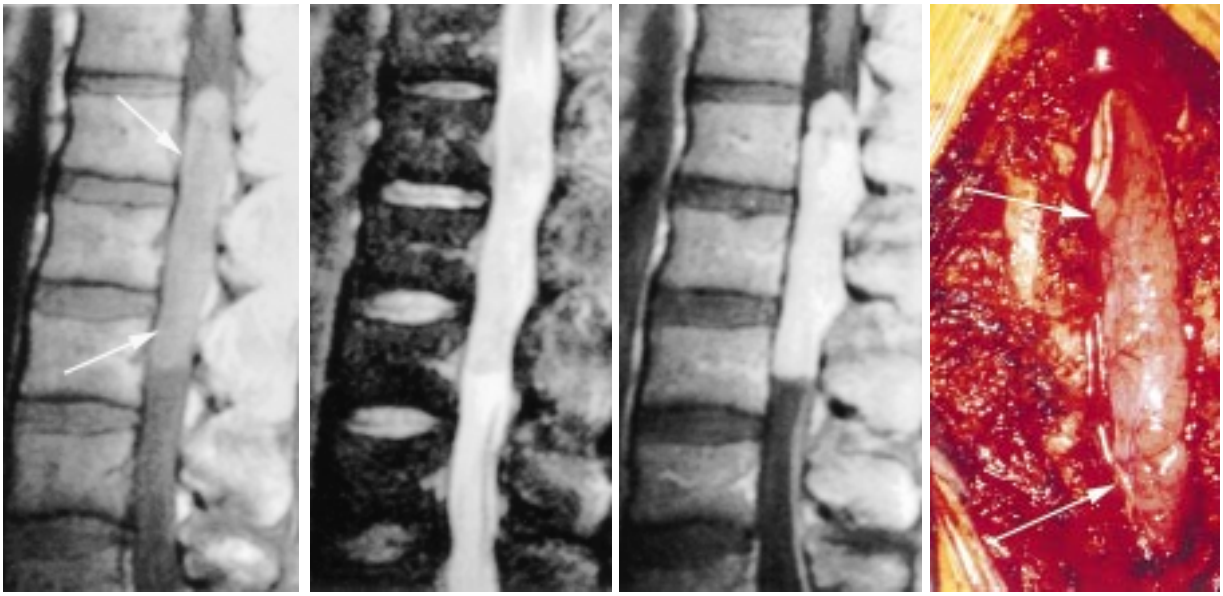

a. b. c. d.

Figure 7. Myxopapillary ependymoma of the filum terminale in a 39-year-old man with chronic low back pain and right leg sciatica. **(a)** Sagittal T1-weighted MR image shows a large intradural oval mass (arrows) extending from the conus medullaris to L3. It is isointense to slightly hyperintense relative to the spinal cord. **(b)** Sagittal T2-weighted MR image reveals mixed signal intensity within the mass. **(c)** Contrast-enhanced sagittal T1-weighted MR image demonstrates intense enhancement of the lesion. **(d)** Intraoperative photograph demonstrates the lobulated, oval intradural mass (arrows). An attachment to the filum terminale was noted at surgical resection.

or sphincter dysfunction. Although most of these tumors are slow growing, those located near the sacrum may be more aggressive, creating large, lytic areas of bone destruction (27,40,41).

Myxopapillary ependymomas are characteristically lobulated, soft, sausage-shaped masses that are often encapsulated (38). The histologic hallmark is heterogeneity, resulting from generous mucin production and papillary zones mixed with cellular areas composed of rosettes and pseudorosettes (Fig 6) (38).

Myxopapillary ependymomas have a nonspecific radiologic appearance and are typically isointense relative to the spinal cord on T1-weighted MR images and hyperintense on T2-weighted MR images. Hyperintensity on both T1- and T2-weighted images may be noted occasionally, a finding that reflects mucin content or hemorrhage (36). Superficial siderosis may be seen but is not specific, as it has been noted in association with other highly vascular tumors (42). Enhancement is virtually always seen after the intravenous administration of contrast material (Fig 7). The predilection of these tumors for the conus medullaris should be suggestive of the diagnosis (39).

Subependymoma

Subependymomas represent a variant of CNS ependymomas that may also occur in the spinal cord (43–45). Originally thought to arise from the pluripotential cells of the subependymal plate (45), these tumors are now believed to have their origin from tanycytes (from the Greek word tanyos, "to stretch"), cells that bridge the pial and ependymal layers (44). Although subependymomas are most commonly found within the ventricular system of the brain, 19 cases of spinal cord subependymomas have been reported in the literature, usually in male patients (74%) and involving at least a portion of the cervical cord. The mean age at presentation is 42 years, and the mean duration of symptoms is 52 months (44). The tumor may recur after surgical resection (46).

Similar to ependymomas, these tumors produce a slowly progressive clinical course with pain as the most common symptom. Sensory and motor dysfunction are reported less frequently. Most patients (83%) in the series reported by Jallo et al (44) had atrophy of one or both distal upper extremities.

a. b. c. d.

Figure 8. Subependymoma of the thoracic spinal cord in a 68-year-old woman with progressive lower-extremity weakness. **(a)** Sagittal T1-weighted image shows ill-defined expansion (arrows) of the lower thoracic spinal cord. The mass is slightly hyperintense relative to the normal spinal cord. **(b)** Sagittal T2-weighted image reveals an abnormal area of high signal intensity (arrow) in the region of the mass. **(c)** Contrast-enhanced sagittal T1-weighted image demonstrates focal enhancement of the mass (arrow). **(d)** Contrast-enhanced axial T1-weighted MR image reveals the eccentric location of the enhancing mass (arrow).

Spinal cord subependymomas are soft gray or grayish yellow masses. The lesions are typically avascular and without evidence of cystic change. At histologic examination, ependymal cells are sparsely dispersed among the predominant fibrillary astrocytes (44).

At MR imaging, they manifest with fusiform dilatation of the spinal cord with well-defined borders. Unlike other ependymomas, they are eccentrically located (Fig 8) (44). In the series of Jallo et al (44), lesions that demonstrated enhancement had sharply defined margins (50% of cases), whereas those that did not enhance had diffuse symmetric spinal cord enlargement. Edema may or may not accompany the main lesion (46). MR imaging findings are not sufficiently unique to enable the differentiation of ependymomas from subependymomas (44,46). A spinal subependymoma may manifest as an extramedullary lesion within the subarachnoid space, perhaps secondary to leptomeningeal heterotopic glial cells (46).

Astrocytoma

Prevalence.—About one-third of all spinal cord gliomas are astrocytomas. Although they are second in prevalence to ependymomas in adults, they are the most common intramedullary tumor in children. Male patients are more commonly afflicted (58% of cases) (1,7,21,24). The mean age at presentation is 29 years (24). The most common site of involvement is the thoracic cord (67% of cases), followed by the cervical cord (49%) (7,18,24). Involvement of the entire spinal cord (holocord presentation) is common in children (up to 60% in one series) but quite rare in adults (18,24). Isolated conus medullaris involvement is seen in about 3% of cases (24). Astrocytomas are rare in the filum terminale and are rarely exophytic (Fig 9) (24).

Clinical Presentation.—Similar to ependymomas, spinal cord astrocytomas most commonly manifest with pain and sensory deficits (53.6% of cases). Motor dysfunction is seen in 41.4% of

Figure 9. Astrocytoma in a 35-year-old woman with lower-extremity weakness and numbness. Contrast-enhanced sagittal T1-weighted MR image demonstrates an irregularly enhancing intramedullary tumor with an enhancing exophytic component (arrowheads).

cases (24). Bowel and bladder deficits are uncommon (24). In the opinion of Epstein et al (5), cord astrocytomas tend to manifest with paresthesia as the sensory deficit, compared with cord ependymomas, which are characterized by dysesthetic features. Objective signs of neurologic dysfunction in lower-grade astrocytomas (grades I and II) are often absent, commonly resulting in delays in the diagnosis. Patients with high-grade lesions (grades III and IV) typically present with symptoms of shorter duration and that progress more rapidly (7,47).

The clinical presentations of young children and adults with comparable astrocytomas differ slightly. Symptoms occur sooner in young children, with a median duration of 5 months (1). Although pain and motor regression are still common, gait abnormalities (27% of cases), torticollis (27%), and scoliosis (24%) are also seen (1). In one series, in patients with holocord involvement, the location of the solid portion of the lesion corresponded with the clinical symptoms (ie, cervical cord location was associated with upper-extremity deficits) (18). These tumors tend to be low-grade astrocytomas, which are characterized by slow growth and low recurrence rates (1). In fact, cord astrocytomas in children tend to behave much like grade I cerebellar pilocytic astrocytomas and displace neural tissue rather than infiltrate it (30). In a review of 100 children with either low-grade astrocytomas or gangliogliomas treated with radical surgery, 95% of patients were alive at 5 years and 80% had a disease-free interval (7). In contrast, more severe neurologic deficit at presentation, hydrocephalus, and leptomeningeal spread of disease were more common in 19 patients with high-grade cord astrocytomas described by Cohen et al (47) than in patients with low-grade tumors. Hydrocephalus alone may be indicative of leptomeningeal spread in the postoperative setting (48).

Adult patients with astrocytomas fare worse than those with cord ependymomas in terms of survival. In Cooper's study of 51 patients with intramedullary spinal cord tumors (30), 11 of 14 (79%) deaths were secondary to astrocytomas. Seven of those 11 patients had high-grade (grade III or IV) astrocytomas and four had low-grade tumors.

Unlike the findings seen in patients with cord ependymomas, the amount of resected astrocytoma did not have an effect on survival. Even in cases of gross total resection, patients with astrocytomas had much higher mortality rates than those with comparable cord ependymomas (30). The poorer prognosis is likely a reflection of the infiltrative nature of astrocytomas for two reasons. First, neoplastic astrocytes extend far beyond the apparent gross tumor margin and provide a source of tumor progression postoperatively. Second, because the malignant cells may extend along the network of normal axonal processes, removal of neoplastic tissue invariably will also necessitate resection of normal functioning cord tissue, which increases the likelihood of postoperative neurologic deficits. There are divergent opinions in the neurosurgical literature about the management of these cases. Some advocate attempts at gross total resection (24), whereas others recommend an initial biopsy of the enlarged cord. If a high-grade astrocytoma is seen at frozen section analysis, tumor debulking is performed. However, knowing that some malignant cells will remain despite gross macroscopic removal and because attempts at gross total resection carry such a high potential

for neurologic morbidity, gross total resection is not necessarily a goal in treating these tumors, and radiation therapy is administered in an attempt to eradicate residual disease (30,49). At least one investigator recommends yearly follow-up MR imaging in all adult patients with cord astrocytomas (30).

Pathologic Characteristics.—At gross inspection, spinal cord astrocytomas are characterized by ill-defined diffuse fusiform enlargement. In contrast to cord ependymomas, a cleavage plane is often not present in most intramedullary spinal astrocytomas (24). Tumor cysts (which are frequently eccentric, smaller, and irregular in shape compared with benign cysts) and syrinxes are common, especially in pilocytic types (32).

All astrocytomas are characterized by hypercellularity and the absence of a surrounding capsule. Accordingly, neoplastic astrocytes will extend along the "scaffold" of normal astrocytes, oligodendrocytes, and axons of the surrounding neural tissue in an infiltrative pattern (32). As a result, astrocytomas are never circumscribed despite an occasional imaging appearance that may suggest otherwise. Enlarged, irregularly shaped, hyperchromatic nuclei are virtually always present at histologic examination.

In general, the amount and degree of pleomorphism correlates with the biologic behavior of these tumors. In the WHO classification, four basic grades of astrocytomas are recognized. Grade I lesions correspond to pilocytic astrocytomas, are commonly seen in the cerebellum (cerebellar cystic astrocytomas), and have the most benign biologic behavior of all the other types. Grade II tumors are of the fibrillary type and are the classic low-grade astrocytoma (Fig 10). Grade III lesions, or anaplastic astrocytomas, contain more pleomorphism, less differentiation, even more hypercellularity, and regions of necrosis compared with the lower-grade lesions. Grade IV lesions, or glioblastoma multiforme, are the most malignant type of astrocytoma and show evidence of endothelial proliferation at microscopic review (Fig 11) (32). Although grade IV lesions make up half of all brain astrocytomas, they are distinctly uncommon in the spinal cord. Only 0.2–1.5% of spinal cord astrocytomas are grade IV lesions. Instead, the well-differentiated grade I astrocytoma (also including gemistocytic and protoplasmic variants) accounts for 75% of cord astrocytomas. Up to 25% of astrocytomas are classified as grade III (anaplastic) lesions. In children younger than 3 years, most cord astrocytomas (80%) are low-grade (either grade I or II) fibrillary types. The remainder are divided between anaplastic (grade III) astrocytomas, glioblastoma multiforme (grade IV), and mixed oligoastrocytomas (1).

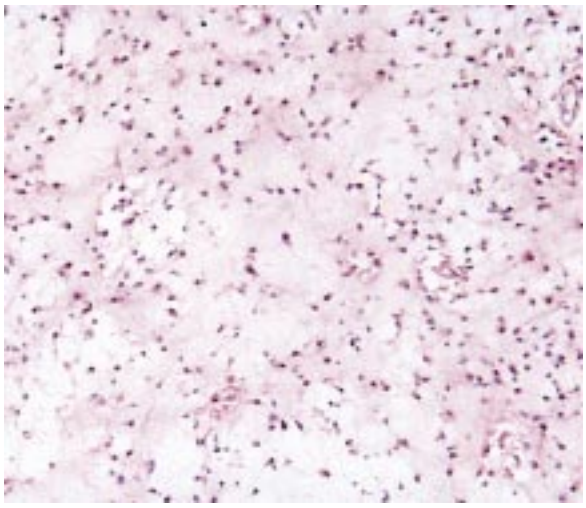

Figure 10. Photomicrograph (original magnification, ×100; H-E stain) of a spinal cord astrocytoma reveals increased cellularity with mild nuclear pleomorphism. The lack of mitotic activity, endothelial proliferation, and necrosis supports the histologic diagnosis of a grade II astrocytoma.

Imaging Characteristics.—Mild scoliosis, widened interpedicular distance, and bone erosion may be seen at conventional radiography and CT, but these signs occur less commonly in astrocytomas than they do in ependymomas. Patients with holocord involvement tend to present

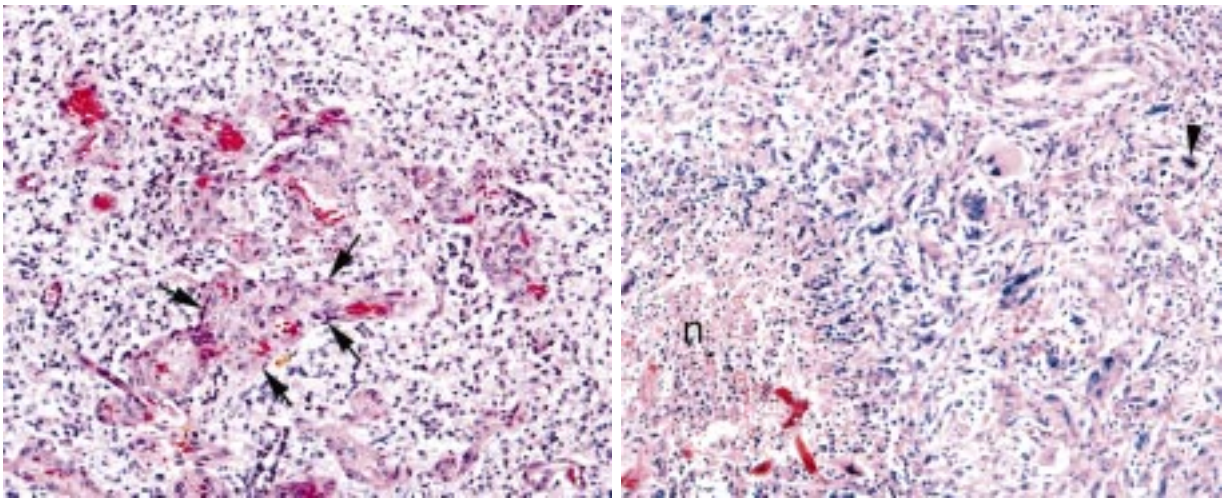

a. **b.**

Figure 11. **(a)** Photomicrograph (original magnification, ×200; H-E stain) of a spinal cord glioblastoma multiforme demonstrates a hypercellular pleomorphic neoplasm with endothelial proliferation (arrows). **(b)** Photomicrograph (original magnification, ×100; H-E stain) of a different field in the same tumor shows zones of necrosis (*n*) and mitotic activity (arrowhead).

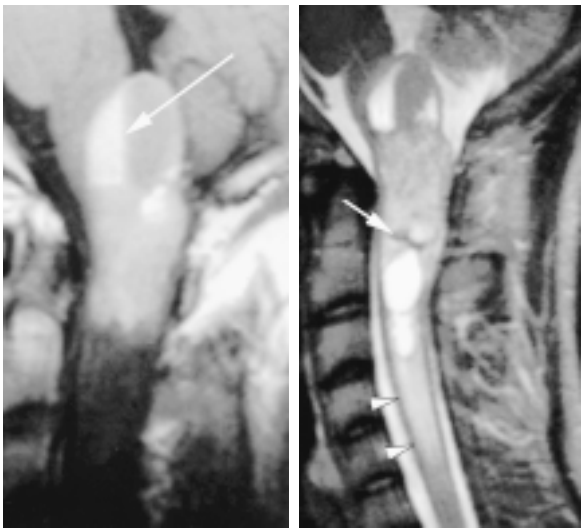

a. **b.**

Figure 12. Intramedullary mixed glioma in a 27-year-old man who presented with neck pain and numbness in his left hand, hiccups, and difficulty in swallowing. **(a)** Sagittal T1-weighted MR image shows an intramedullary, slightly hyperintense, heterogeneous mass of the upper cervical spinal cord extending into the medulla. There is a cystlike area with a fluid-fluid level (arrow). **(b)** Sagittal T2-weighted MR image reveals a heterogeneous intramedullary lesion and a brainstem cyst containing a fluid-fluid level. A curvilinear, low-signal-intensity area within the cord (arrow) is suggestive of hemorrhage. Cord edema (arrowheads) is evident inferior to the mass. The image plane is slightly lateral to that shown in **a**.

with scoliosis and canal widening (18). At MR imaging, these neoplasms usually have poorly defined margins and are iso- to hypointense relative to the spinal cord on T1-weighted images and hyperintense on T2-weighted images. The average length of involvement is seven vertebral segments. Cysts are a common feature, with both polar and intratumoral types being observed (Fig 12) (1). Virtually all cord astrocytomas show at least some enhancement following the intravenous administration of contrast material (1). The cap sign is not associated with cord astrocytomas (16). Because astrocytomas arise from the cord

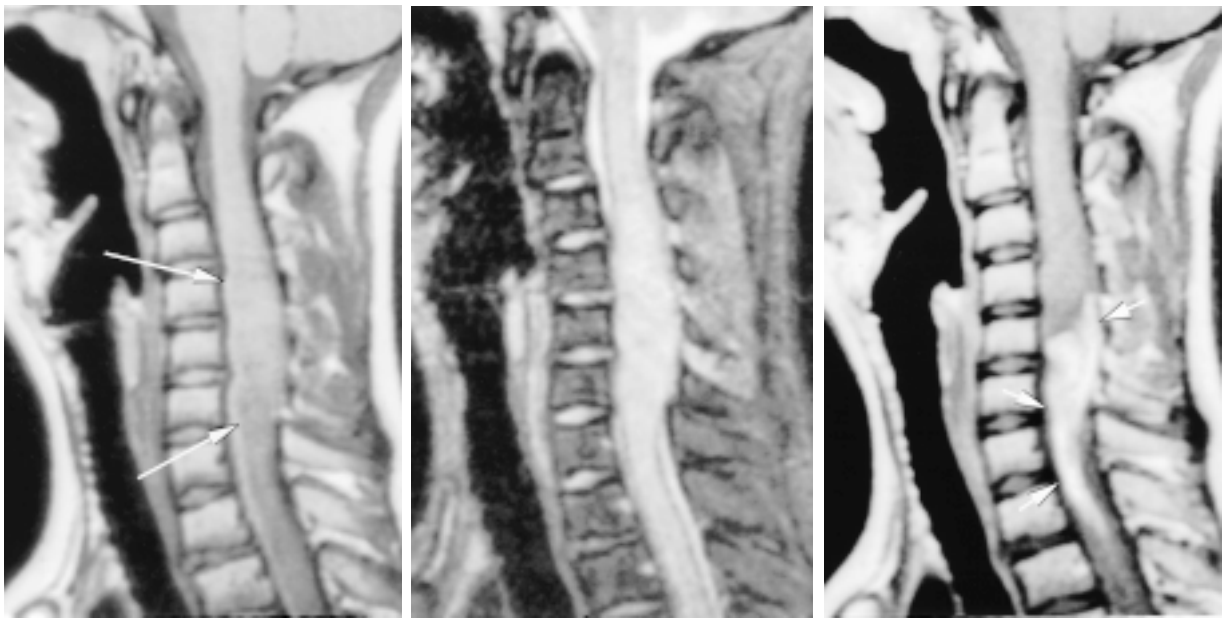

a. b. c.

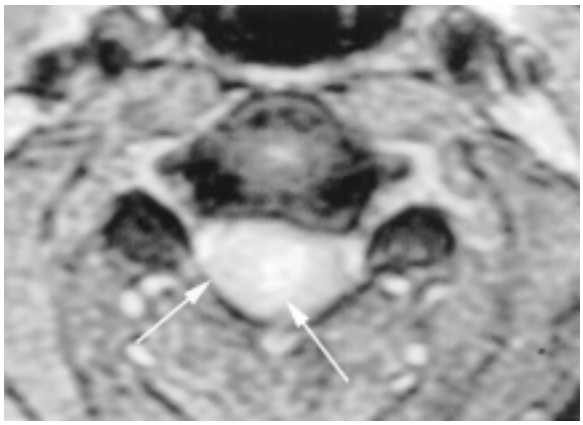

d.

Figure 13. Intramedullary glioblastoma multiforme in a 14-year-old boy who presented with neck pain. **(a)** Sagittal T1-weighted MR image shows irregular expansion of the cervical spinal cord extending from C3 to C7 (arrows). The affected cord is slightly hypointense relative to the unaffected cord. Note expansion of the spinal canal secondary to bony remodeling. **(b)** Sagittal T2-weighted MR image reveals an abnormal area of high signal intensity throughout the expanded region. **(c)** Contrast-enhanced sagittal T1-weighted MR image displays irregular, intense, homogeneous enhancement of the inferior portion of the expanded cord from C5 through T1 (arrows). **(d)** Axial gradient-echo MR image demonstrates expansion of the cord with the mass eccentrically located along its right margin (arrows).

parenchyma and not from the central canal, they are usually (57% of cases) eccentric within the cord (Fig 13) (16). Leptomeningeal spread is seen in 60% of intramedullary glioblastoma multiformes (47,50). At transverse imaging, intraoperative US reveals asymmetric expansion of the spinal cord with variable echogenicity. Frequently, the lesion is virtually isoechoic relative to the normal spinal cord (17).

A summary of the salient features of spinal cord ependymomas and astrocytomas is provided in Table 2.

Ganglioglioma

Prevalence.—Gangliogliomas account for 0.4%–6.25% of all primary CNS tumors and about 1.1% of all spinal neoplasms (51). They are more common in children than in adults, with 19 years of age being the mean age of presentation (51). There is no gender predilection (51,52). Within the CNS, most gangliogliomas are located supratentorially, primarily arising in the temporal lobe. In rare cases, they may extend into the cervical spinal cord from the cerebellum (53). In a review of 22 spinal cord tumors with a

Table 2
Characteristics of Ependymoma and Astrocytoma

Characteristic	Ependymoma	Astrocytoma
Population in which lesions most commonly occur	Adult	Pediatric
Location in the spinal canal	Central	Eccentric
Morphologic appearance	Well circumscribed	Ill defined
Hemorrhage	Common	Uncommon
Enhancement with contrast material	Focal, intense homogeneous	Patchy, irregular
Predilection for involvement of the conus medullaris or filum terminale	Yes	No

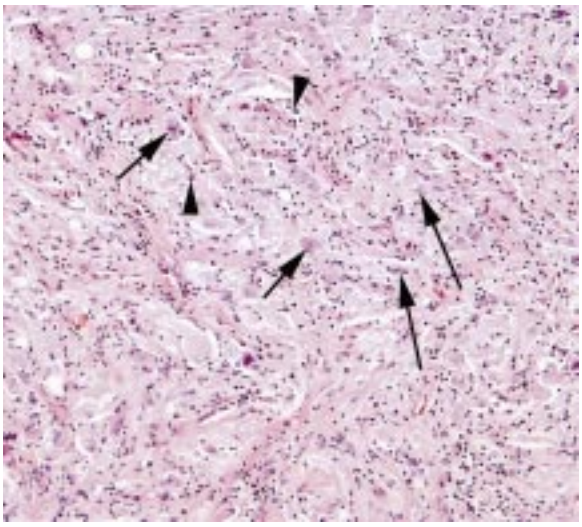

Figure 14. Photomicrograph (original magnification, ×100; H-E stain) of a spinal cord ganglioglioma shows groups of irregular ganglion cells (short arrows) and neoplastic glial cells (long arrows) with scattered lymphocytes (arrowheads).

known location, there was near-equal distribution between the cervical and thoracic regions (51). Patel et al (52) reported that almost half of their 27 cases (48%) arose within the cervical cord, with the thoracic cord a distant second (22%). Less commonly, gangliogliomas may involve the conus medullaris or the entire spinal cord (holocord) (51,52). They are commonly eccentric in location and contain tumoral cysts even more often (46% of cases) than do spinal astrocytomas (20%) and ependymomas (3%) (51,52).

Clinical Presentation.—As with ependymomas, gangliogliomas are characterized by slow growth and a good prognosis. Rarely, malignant forms may occur and disseminate through the CNS (54). There is a wide range in duration of symptoms (1 month to 5 years) (51). Although the potential for malignancy is low, spinal cord gangliogliomas have a recurrence rate of 27%, which is about three to four times that of cerebral gangliogliomas (51). Overall, patients with spinal gangliogliomas have a 5-year survival rate of 89% and a 10-year survival rate of 83% (51).

Pathologic Characteristics.—True to their name, gangliogliomas represent a mixture of mature but neoplastic neuronal elements (neurons or ganglion cells) and glial elements (primarily neoplastic astrocytes) at histologic examination (Fig 14). Because the proportions of cells may vary from tumor to tumor, various synonyms have been used to describe these lesions, including ganglioglioneuroma, ganglionic neuroma, neuroastrocytoma, neuroganglioma, ganglionic glioma, neuroma gangliocellulare, and neuroglioma (52). The neuronal cells are typically irregularly oriented and arranged in clusters. As with normal neuronal cells, the neoplastic neuronal cells in spinal cord gangliogliomas demonstrate immunopositivity for synaptophysin. Other immunohistochemical stains (neurofilament protein, neuron-specific enolase, and chromogranin A) are also frequently positive. Nonspecific histologic features (Rosenthal fibers, eosinophilic

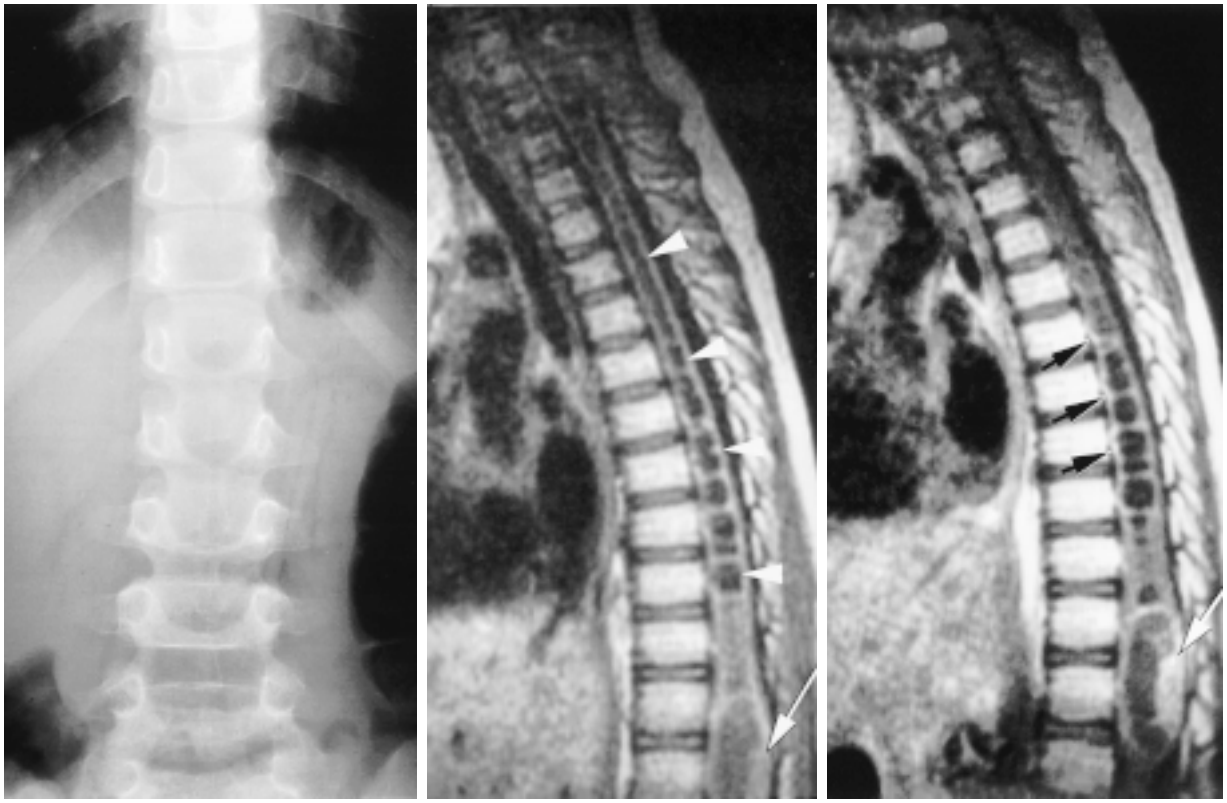

a. b. c.

Figure 15. Ganglioglioma in a 7-year-old boy with abdominal pain. **(a)** Frontal radiograph demonstrates a widened interpedicular space, which is suggestive of an intraspinal lesion. **(b)** Sagittal T1-weighted MR image of the spine shows expansion of the lower thoracic cord and conus medullaris region with an associated syringohydromyelia (arrowheads) and an irregularly thickened posterior wall (arrow). **(c)** Contrast-enhanced sagittal T1-weighted MR image demonstrates enhancement of the posterior thickening in the distal cord (white arrow) and along the anterior margin of the midthoracic cord (black arrows).

granular bodies) are common (51). Accordingly, these tumors are classified as grade I or II lesions in the WHO system. Calcification and small cysts are common (55). Malignant transformation in CNS gangliogliomas has been reported in the literature (about 10% of cases) and may be related to prior irradiation (54). There are no histologic markers that enable the prediction of biologic behavior (51). It is speculated by some that spinal gangliogliomas have been underdiagnosed in the past, being labeled as astrocytomas or other tumors (52). However, not all investigators share this opinion (56).

Imaging Characteristics.—Osseous changes including scoliosis (44% of cases) and remodeling (93%) are much more common in spinal gangliogliomas than in other tumor types (Fig 15) (52). These tumors have a wide range of signal intensities on MR images. In the study by Patel et al (52), most tumors (84%) had mixed signal intensity on T1-weighted images. In their opinion, this feature was somewhat unique for spinal neoplasms and was uncommonly seen in cord ependymomas or astrocytomas. Patel et al speculated that the mixed signal intensity may be caused by the dual cellular population (ie, neuronal and glial elements). Tumors that are hyperintense, hypointense, and isointense relative to the spinal cord, however, can also be seen (51, 52). Gangliogliomas have high signal intensity, usually of a homogeneous nature, on T2-weighted images (51,52). Surrounding edema is less commonly seen in spinal gangliogliomas than in cord ependymomas or astrocytomas (52). Calcification evidently occurs much less frequently in spinal gangliogliomas than in intracranial gangliogliomas, since only one of the 27 cases in the study

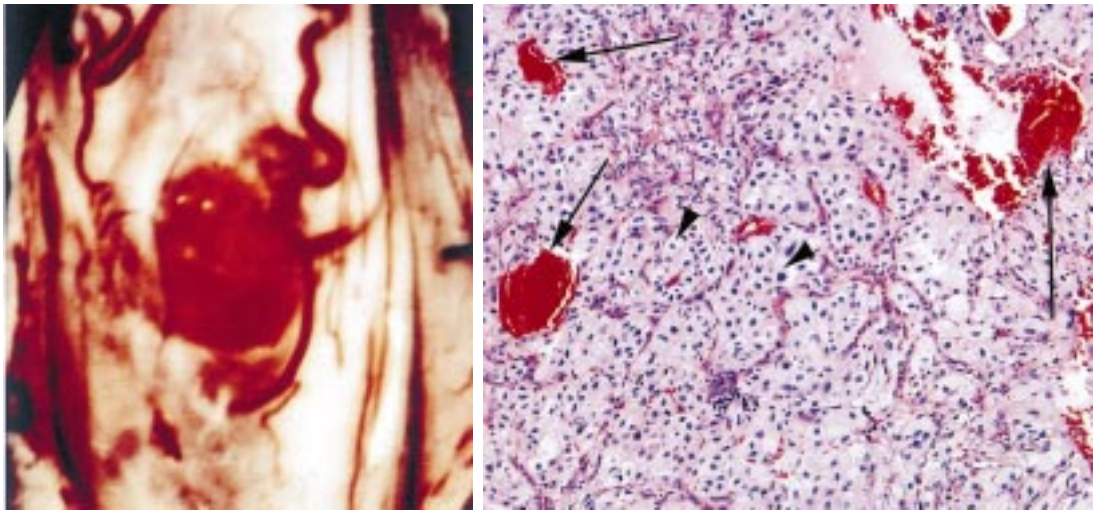

a. **b.**

Figure 16. Hemangioblastoma of the conus medullaris. **(a)** Intraoperative photograph demonstrates a vascular mass with enlarged draining veins. **(b)** Photomicrograph (original magnification, ×100; H-E stain) of a spinal cord hemangioblastoma demonstrates a hypervascular neoplasm with prominent zones of hemorrhage (arrows) and densely packed large stromal cells with hyperchromatic nuclei (arrowheads).

by Patel et al (52) had a focus of magnetic susceptibility suspected to be a calcified area. The vast majority of spinal gangliogliomas enhance to at least some degree after the administration of contrast material. Patchy enhancement is the most common pattern (65% of cases), but enhancement of the pial surface is also common (58%) (Fig 15c). Approximately 15% of these lesions show no enhancement (51,52).

Nonglial Neoplasms

Hemangioblastoma

Prevalence.—Hemangioblastomas constitute 1.0%–7.2% of all spinal cord neoplasms and show no gender predilection (24,57,58). Although most of these tumors (75%) are intramedullary, they may involve the intradural space or even be extradural. Extramedullary hemangioblastomas are commonly attached to the dorsal cord pia or nerve roots (41,59). These slowly growing lesions involve the thoracic cord most commonly (50% of cases), followed closely by the cervical cord (40%) (41, 60). Most cord hemangioblastomas (80%) are solitary and occur in patients younger than 40 years, usually with impaired proprioception (41). Multiple lesions indicate the manifestation of von Hippel–Lindau syndrome (61).

Clinical Presentation.—Symptoms of sensory changes (39% of cases), motor dysfunction (31%), and pain (31%) commonly accompany hemangioblastomas. As with other primary intramedullary spinal neoplasms, a long clinical course is the rule, with a mean symptom duration of 38 months. One-third of patients have von Hippel–Lindau syndrome, with retinal or cerebellar findings usually preceding spinal cord manifestations (41,57,60,62). Rarely, spinal hemangioblastomas may be a source of subarachnoid hemorrhage or hematomyelia (60,63–66).

Pathologic Characteristics.—At gross examination, cord hemangioblastomas most commonly appear as highly vascular, discrete, nodular, red-to-orange masses abutting the leptomeninges with prominent dilated and tortuous vessels on the posterior cord surface (Fig 16a) (24,57,58,67). An associated syrinx is common (58,67). Occasionally, the tumor may exophytically extend from the spinal cord (68,69). The cell of origin remains a mystery (67). Histologic examination reveals large, pale stromal cells packed between blood vessels of varying size. These stromal cells dominate the cellular portions of these benign neoplasms (Fig 16b) (67).

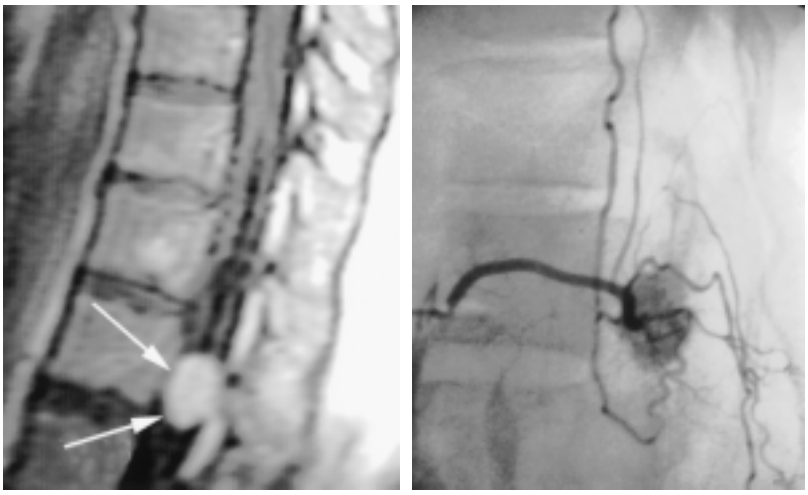

a. b.

Figure 17. Hemangioblastoma of the conus medullaris. **(a)** Contrast-enhanced sagittal T1-weighted MR image demonstrates a well-circumscribed oval mass (arrows) with intense enhancement. **(b)** Spinal angiogram shows the hypervascular mass with a prominent feeding artery and draining vein.

Imaging Characteristics.—Dilated tortuous feeding arteries and draining pial veins are seen on half of the conventional myelographic studies (70). Unenhanced CT may reveal a hypoattenuated cystlike mass (71). A highly vascular mass, dense prolonged blush, and prominent draining veins are noted at diagnostic angiography (Fig 17b) (41,62).

Hemangioblastomas manifest with diffuse cord expansion and variable signal intensity on T1-weighted images, with the most common appearance being isointense (50% of cases) or hyperintense (25%) relative to the normal spinal cord. On T2-weighted images, these lesions characteristically have high signal intensity with intermixed focal flow voids (41), although other reports found that the mass was not even detectable in 33% of cases (24). Surrounding edema and a cap sign may also be seen (16,24). Although up to 25% of hemangioblastomas may appear to be solid, cyst formation or syringohydromyelia is very common (up to 100% in some series) (24,57,58,72). In fact, some cases may have the classic "cystic mass with an enhancing mural nodule" appearance characteristic of cerebellar hemangioblastomas (72). Contrast-enhanced cross-sectional imaging typically shows an intensely homogeneous enhancing tumor nodule (Fig 17) (41,62,69,72,73).

Three-dimensional phase-contrast MR angiography may provide important noninvasive preoperative information by demonstrating greater detail in the architecture of the feeding vessels than is possible with other MR angiographic sequences (74). Screening MR imaging of the brain and spine is recommended for patients with a positive family history of von Hippel–Lindau syndrome (60,62). The presence of a well-defined mass and homogeneous signal intensity facilitates the differentiation of these lesions from spinal arteriovenous fistulae, which may otherwise mimic a spinal cord hemangioblastoma at imaging (6).

Paraganglioma

Prevalence.—Paragangliomas are neoplasms of neuroendocrine origin, arising from specialized organelles called paraganglia, the accessory organs of the peripheral nervous system. Most commonly, these tumors are located within the adrenal gland (pheochromocytomas), the carotid body at the common carotid artery bifurcation (carotid body tumors), the jugular foramen (glomus jugulare tumors), or the immediate proximity of the vagus nerve (vagal paragangliomas) (75). These tumors may also arise in several other sites throughout the body. Lerman et al (76) first described the spinal paraganglioma of the filum terminale in 1972.

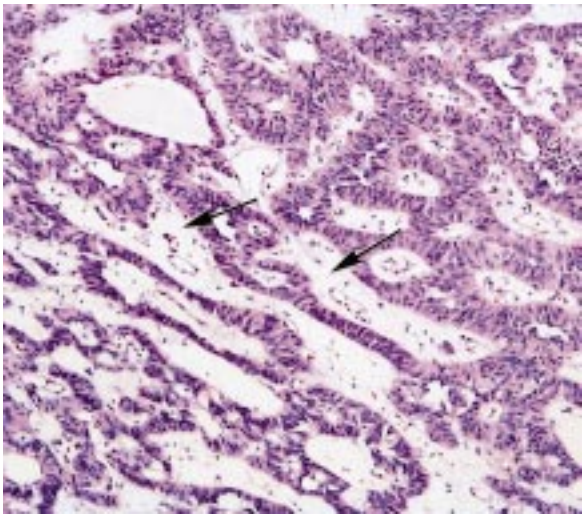

Figure 18. Photomicrograph (original magnification, ×100; H-E stain) of a spinal cord paraganglioma reveals relatively uniform polygonal chief cells and fibrovascular stroma (arrows). The combination of these features creates an overall trabecular pattern.

Clinical Presentation.—Spinal paragangliomas are almost always located in the intradural extramedullary compartment, with a definite affinity for the cauda equina and filum terminale (77). Consequently, they typically manifest as lower back pain and sciatica. As with other spinal neoplasms described herein, a long duration of symptoms is typical (mean, 4 years) (78). Paragangliomas are slightly more common in male patients, and the average age at presentation is 46 years. The average tumor size is 3.3 cm (range, 1.5–10.0 cm) (78). Cauda equina paragangliomas frequently actively secrete neuropeptides, particularly 5-hydroxytryptamine and somatostatin, although symptoms related to this chemical production are usually absent (79). The lesion may also be a rare source of superficial siderosis (80,81).

Pathologic Characteristics.—At gross inspection, paragangliomas are typically soft masses that are encapsulated and homogeneous but slightly hemorrhagic (77,82). Prominent vascularity in the form of numerous feeding arteries is common, and paragangliomas occasionally form a pedicular attachment to a nearby nerve root or the filum terminale (82). Paragangliomas have a biphasic histologic pattern composed of chief cells and sustentacular cells, both of which are surrounded by a fibrovascular stroma (Fig 18) (83). The histologic features of spinal paragangliomas are similar to those of paragangliomas located elsewhere in the body, and they characterized by nests of chief cells in the classic "zellballen" (cell ball) configuration. Prominent vascular channels are typical in these highly vascular tumors. Areas of melanin and spindle cell proliferation may be seen occasionally (77). Although paragangliomas can be locally aggressive, bone erosion and distant metastasis are not common (79).

Immunohistochemical techniques increase the diagnostic accuracy, but, to date, the histologic diagnosis rests with careful examination of slides with conventional stains (75). Most spinal paragangliomas (75%) are encapsulated, correlating with a decreased rate of recurrence. When they are unencapsulated, recurrences are much more common (84).

Imaging Characteristics.—Despite dozens of articles about spinal paragangliomas in the pathology and neurosurgery literature, there are only scattered case reports of imaging findings in these lesions in radiology journals (79,85–90). Bone erosion, when it occurs, is easily detected on CT images (79). Conventional angiographic

images reveal an intense early blush that persists well into the late arterial and early venous phases (79). MR imaging studies of these lesions typically reveal a well-circumscribed mass that is isointense relative to the spinal cord on T1-weighted images and iso- to hyperintense on T2-weighted images (Fig 19) (87–89). Hemorrhage is common, and a low-signal-intensity rim (cap sign) may be seen on T2-weighted images. In some lesions, the characteristic "salt-and-pepper" appearance, which is so common in neck and skull base paragangliomas, may also be seen (89). Intense enhancement of these highly vascular lesions is virtually always seen after the administration of contrast material. Serpentine flow voids along the surface and within the tumor nodule are typical (87–89). Associated syringohydromyelia has been reported in some cases (89,90).

Metastasis

Prevalence.—Intramedullary spinal metastases are rare, occurring in only 0.9%–2.1% of autopsied cancer patients (91). They are most commonly located in the cervical cord (45% of cases), followed by the thoracic cord (35%) and the lumbar region (8%) (92). Most metastases are solitary, with an average length of two to three vertebral segments (93). Lung carcinoma (40%–85% of cases) is the most common primary site, followed by breast carcinoma (11%), melanoma (5%), renal cell carcinoma (4%), colorectal carcinoma (3%), and lymphoma (3%); 5% of the primary sites are unknown (92). Cerebellar medulloblastoma has also been recorded as a causative source (94,95). Documented routes of spread include hematogenous (via the arterial supply) and direct extension from the leptomeninges (91,96). Dissemination through the central canal of the spinal cord was suspected in two cases reported in the literature (94,95). Extension along the Batson venous plexus for retroperitoneal primary tumors or extension along perineural lymphatic ducts is also a theoretic possibility (91).

Clinical Presentation.—Virtually all patients have motor weakness. Pain (70% of cases), bowel or bladder dysfunction (60%), and paresthesia (50%) are other common clinical manifestations. A rapid decline in neurologic status in an elderly patient is typical. In contrast to the long duration of symptoms that accompany primary intramedullary spinal neoplasms described elsewhere in this article, most patients with a spinal cord metastasis (75%) have symptoms for less than 1 month before diagnosis (92). The prognosis for patients with intramedullary metastases is dismal: Two-thirds of these patients die within 6 months. Until recently, radiation therapy was advocated as the only treatment for these patients with systemic disease. Some investigators, however, have recommended microsurgical resection for discrete, well-defined lesions to improve the quality of remaining life (92). Radiation therapy and corticosteroid therapy are still the treatments of choice for metastasis from a radiosensitive primary tumor or in the setting of diffuse and widespread disease (92).

Imaging Characteristics.—Radiographs are usually normal in patients with intramedullary spinal metastases. Even with myelography, up to 40% of cases are undetected (92). This is not surprising given that in four of 13 patients in a series reported by Costigan and Winkelman (91), metastases were visible only with microscopy and were clinically silent. Post et al (97) had better success demonstrating these lesions as definite intramedullary expansion with myelography and CT. MR imaging was clearly superior to these other modalities, however, and often revealed clinically unsuspected additional lesions (97). Lesions typically produce mild cord expansion over several segments. On T1-weighted images, a central area of low signal intensity (mimicking a syrinx) may be seen. On T2-weighted images, high signal intensity (reflecting edema or tumor infiltration) is typical. Cysts are rare, in contrast to

Figure 19. Paraganglioma of the cauda equina in a 33-year-old woman with neurogenic claudication and an unsteady gait. **(a)** Sagittal T1-weighted image shows a homogeneous, oval, well-circumscribed mass (arrows) at the L2 level. The mass is hyperintense relative to the spinal cord. **(b)** Contrast-enhanced sagittal T1-weighted MR image demonstrates intense but mildly heterogeneous enhancement of the mass. **(c)** Sagittal T2-weighted MR image reveals that the mass is slightly hyperintense relative to the cerebrospinal fluid. The "cap sign" (arrowheads), which is indicated by the low-signal-intensity rim, is also seen. In this particular case, this appearance could be secondary to a fibrous capsule, hemorrhage, or a combination of these features. **(d)** Photograph of the resected specimen demonstrates a hemorrhagic encapsulated mass. **(e)** Contrast-enhanced axial T1-weighted MR image shows heterogeneous signal intensity with focal nonenhancing regions, which is suggestive of either central necrosis or cystic degeneration. **(f)** Bisected specimen reveals a hemorrhagic internal cystic region, which corresponds to the axial imaging findings.

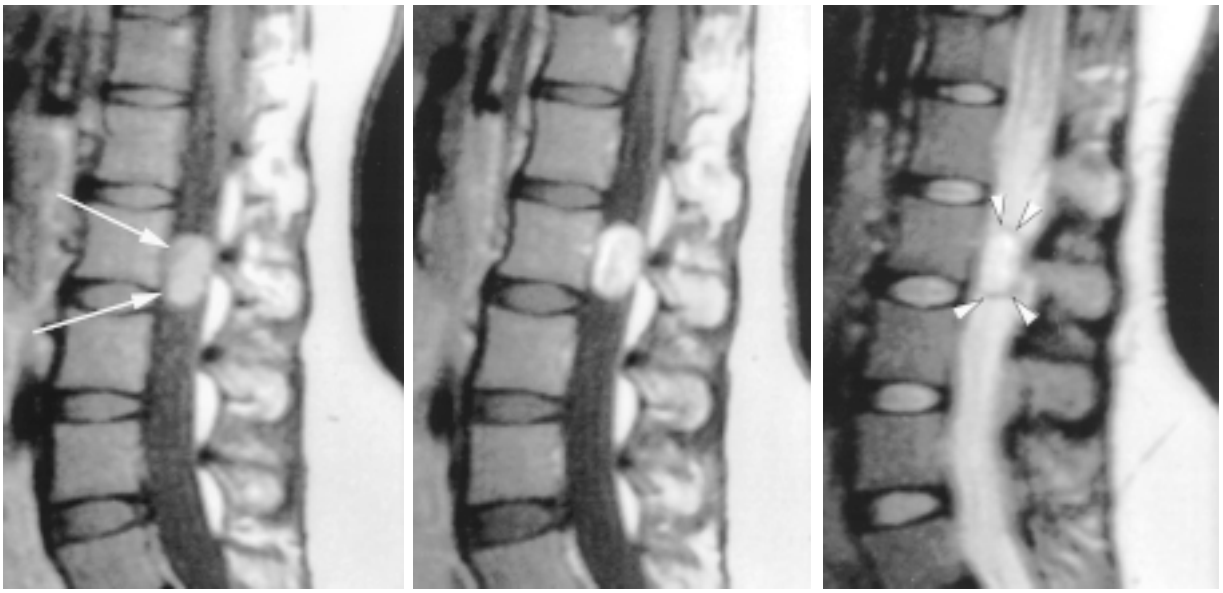

a. **b.** **c.**

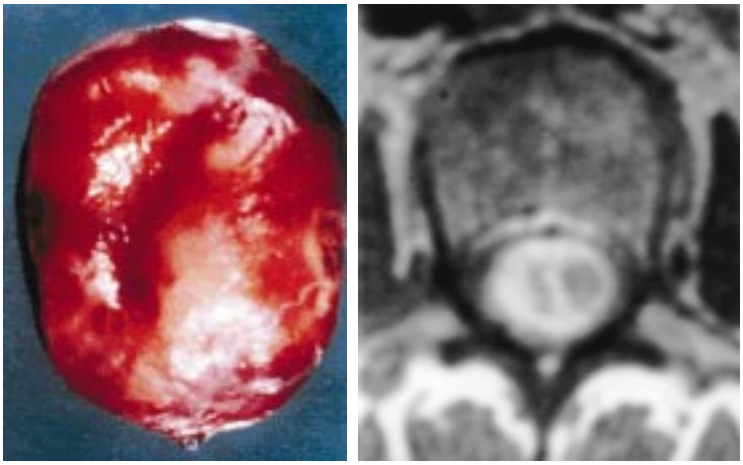

d. **e.**

f.

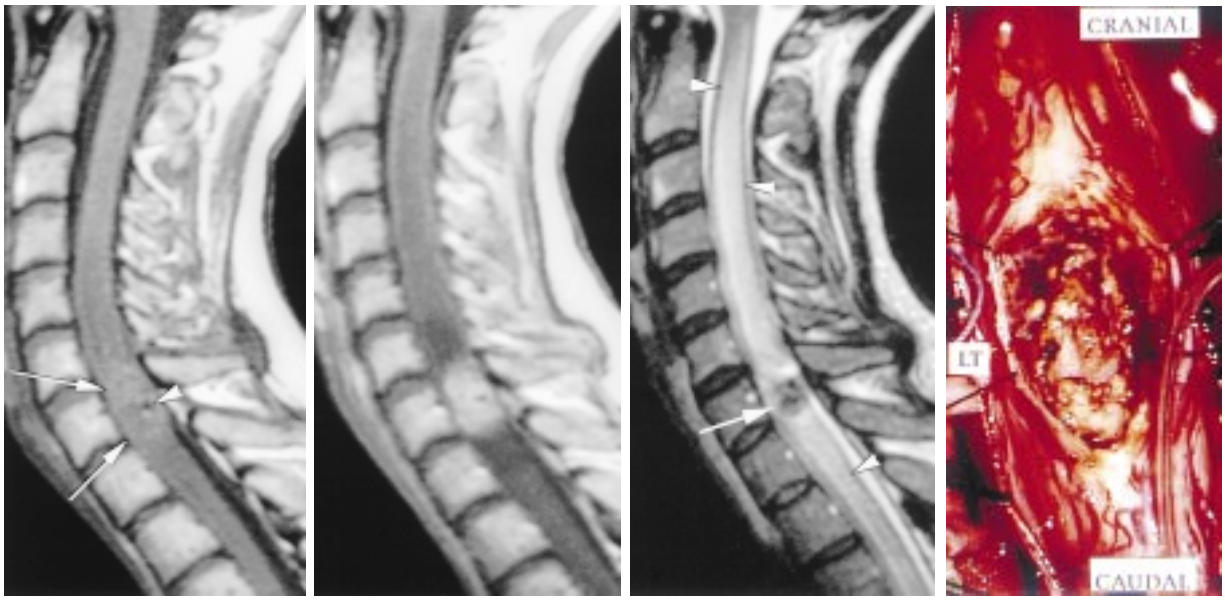

a. b. c. d.

Figure 20. Intramedullary metastasis from infiltrating ductal carcinoma of the breast in a 35-year-old woman with numbness of the lower extremities and bowel and bladder dysfunction. **(a)** Sagittal T1-weighted MR image shows a mass (arrows) that is slightly hyperintense relative to the surrounding spinal cord at the cervicothoracic junction, with mild cord expansion. There is extensive edema around the lesion. A punctate area of low signal intensity (arrowhead), which is suggestive of either calcification or focal hemorrhage, is also seen at the C7 level. **(b)** Triple-dose contrast-enhanced sagittal T1-weighted MR image demonstrates moderate enhancement of the mass. **(c)** Sagittal T2-weighted MR image reveals the well-circumscribed low-signal-intensity mass (arrow). Cord edema (arrowheads) extends from the mass. **(d)** Intraoperative photograph demonstrates the intramedullary mass with an internal area of old hemorrhage corresponding to imaging findings.

primary intramedullary neoplasms. Cord metastases enhance intensely and homogeneously, with generous amounts of surrounding edema, often disproportionately increased for the size of the lesion (Fig 20) (13).

Lymphoma

Prevalence and Clinical Features.—Although most cases of spinal lymphoma involve the epidural compartment and bony vertebra, lymphoma may also be confined to the spinal cord. Intramedullary spinal lymphoma accounts for only 3.3% of CNS lymphoma, which constitutes only 1% of all lymphomas in the body (98). Clinical presentation typically includes weakness, numbness, and progressive difficulty in ambulation (99–102). Of at least 15 cases reported in the literature, the cervical cord is the most commonly affected site, followed by the thoracic cord and the lumbar region (99–105). Most lymphomas are solitary. There is a slight female predominance, and the mean age at presentation is 47 years. Patients with primary intramedullary spinal lymphoma may have a better prognosis than those with primary intracranial CNS lymphoma (104).

Pathologic Characteristics.—At histologic examination, CNS lymphoma is characterized by a monotonous collection of lymphocytes packed tightly into the perivascular space (Fig 21). Immunohistochemical stains aid in the identification of a predominant population of B-cell lymphocytes and help establish the diagnosis (98). However, three of the reported cases in the literature proved to have a T-cell lineage (99,100, 106), which is an unusual feature in CNS lymphoma in which B-cell lymphocytes dominate the cellular population. It is speculated that myelopathy associated with human T-cell lymphotropic virus type I may be a precursor to T-cell spinal cord lymphoma (100).

Imaging Characteristics.—There are only a few reports of MR imaging findings in intramedullary lymphoma. It is noteworthy that all spinal

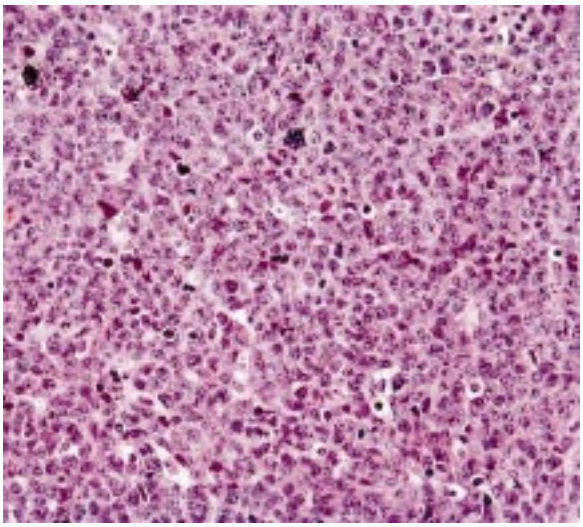

Figure 21. Photomicrograph (original magnification, ×200; H-E stain) of a spinal cord lymphoma demonstrates a monotonous sheet of atypical large lymphocytes. Immunohistochemical staining revealed that the vast majority of these cells are of B-cell origin.

a. **b.**

Figure 22. Intramedullary spinal lymphoma. **(a)** Sagittal T1-weighted MR image shows an ill-defined region of slightly high signal intensity (arrows) in the midthoracic spinal cord. **(b)** Sagittal T2-weighted MR image reveals abnormal high signal intensity (arrow) in the same region. Extensive cord edema (arrowheads) is also seen.

cord lymphomas had high signal intensity on T2-weighted images, in contrast to the characteristic low signal intensity seen in intracranial lesions at T2-weighted imaging (Fig 22). Bluemke and Wang (101) reported a case with fusiform expansion of the cervical cord. The lesion was isointense relative to the spinal cord on T1-weighted images, hyperintense on T2-weighted images, and enhanced intensely after contrast material administration. Caruso et al (102) described a case of multicentric intramedullary spinal lymphoma associated with cervical spinal stenosis in a 77-year-old man who presented with clinical features of spondylitic myelopathy. The lesion was hyperintense relative to the spinal cord on T2-weighted images. A corresponding focal area of eccentric enhancement was seen along the dorsal cord margin after administration of gadolinium-based contrast material. A separate enhancing area was also present within the thoracic cord. Schild et al (99) reported a case involving the distal thoracic cord in which the lesion was isointense relative to the spinal cord on unenhanced T1-weighted images and intensely homogeneously enhanced after contrast material administration. A fourth case involving the distal spinal cord had mixed signal intensity on T1-weighted images and hyperintensity on T2-weighted images. There was irregular enhancement following contrast material administration (100).

Primitive Neuroectodermal Tumor

Prevalence.—Most cases of PNET involving the spinal axis are secondary to subarachnoid seeding, which leads to leptomeningeal deposits (so-called drop metastasis from an intracranial primary tumor) along the nerve roots or pial surface of the spinal cord. To our knowledge, only 20 cases of primary spinal PNETs have been reported in the literature (107–113). Locations include the spinal cord, intradural-extramedullary compartment including the cauda equina, and the extradural compartment (107,114). One of the cases reported manifested as an exophytic mass that mimicked an extramedullary lesion (110). Unlike intracranial PNETs, those involving the spine are slightly more common in adults than in children. Most cases (60%) have occurred in male patients (107–113). Clinical presentation is nonspecific, with weakness, paresthesias, gait disturbance, and pain being the most common symptoms (107,109,110,114). These aggressive lesions frequently recur and can disseminate through the cerebrospinal fluid, even producing intracranial lesions from the spinal primary site (115). Distant metastatic spread from the spinal lesions may also occur to the usual sites for PNET dissemination

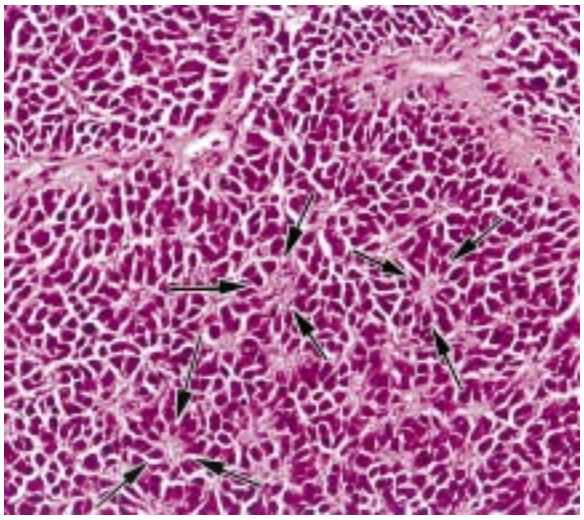

Figure 23. Photomicrograph (original magnification, ×200; H-E stain) of a spinal cord PNET shows numerous small, round, blue cells with scant cytoplasm and hyperchromatic nuclei. Several Homer-Wright rosettes (arrows) are also seen.

a. **b.**

Figure 24. Intramedullary PNET in a 14-month-old boy with grand mal seizures, developmental delay, and lower-extremity paraplegia. **(a)** Sagittal T1-weighted MR image shows a large holocord mass with septations and expansion of the cord, particularly near the conus medullaris. **(b)** Contrast-enhanced sagittal T1-weighted MR image demonstrates the diffusely enhancing holocord intramedullary mass (arrows). The more distal thoracic cord does not enhance, which suggests that the dilatation of this region is secondary to syringohydromyelia.

(lungs, bones, and lymph nodes). Similar to intracranial PNETs and despite a therapeutic combination of surgery, radiation therapy, and chemotherapy, spinal PNETs carry a poor prognosis. More than half of the patients died from the disease within 2 years of diagnosis (107).

Pathologic Characteristics.—The classification of these tumors is controversial (116). The most recent WHO classification lists them as "embryonal tumors," with PNET used as a generic term for cerebellar medulloblastoma and other similar-appearing tumors arising within the supratentorial compartment (117). Still, there are ardent defenders of the concept of PNET as a unique classification for a group of neoplasms that are believed to share a common cellular ancestry from primitive undifferentiated cells and that are distinguished from each other only by their location within the CNS and the degree and type of differentiation contained within each one (118,119). Numerous small round blue cells with hyperchromatic nuclei and scanty cytoplasm and frequent mitotic figures dominate the histologic picture in these tumors (Fig 23).

Imaging Characteristics.—The few cases reported in the literature were not visualized at unenhanced CT. A complete block at the conus medullaris may be seen at CT myelography. MR imaging features are nonspecific, with T1 and T2 prolongation (Fig 24). Recently, 2-[fluorine-18] fluoro-2-deoxy-D-glucose positron emission tomography depicted a case of recurrent spinal PNET as a hypermetabolic focus (109). One case occurred in a child with numerous neuroskeletal anomalies (vertical talus, pectus excavatum, hip dislocation, sacral dysgenesis, and distorted neural arches) suggestive of a neural tube defect (120).

Other Spinal Cord Masses

Although the vast majority of lesions responsible for an expanded spinal cord are of either glial or intramedullary nonglial origin, common extramedullary neoplasms and other nonneoplastic diseases can occasionally manifest as an intramedullary spinal mass. Salvati et al (121) reported four cases of intramedullary meningiomas, all occurring in the cervical spinal cord. Intramedullary schwannomas also rarely occur (Fig 25) (20,122). All reported cases have been located in the posterior half of the spinal cord, and one tracked along a sensory nerve root into the spinal cord. It is believed that these nerve sheath tumors probably arise along the posterior nerve root at the point where it loses its Schwann cell sheath at the pia-arachnoid margin of the cord. There are numer-

a.

b.

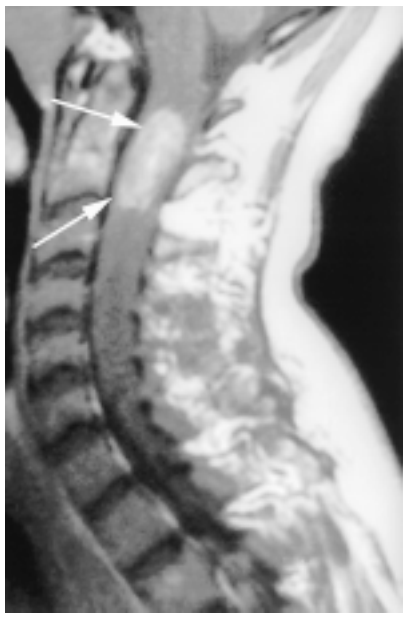

c.

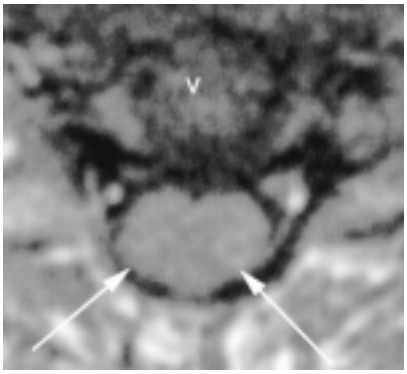

d.

Figure 25. Intramedullary schwannoma in a 24-year-old man with progressive upper-extremity weakness and numbness. **(a)** Sagittal T1-weighted MR image shows mild expansion of the upper cervical cord at C1-C2, with subtle ill-defined mild high signal intensity extending into the medulla. **(b)** Sagittal T2-weighted MR image reveals diffuse increased signal intensity in the affected region of the cord extending inferiorly. The mass (arrows) at C1-C2 level has slightly high signal intensity and a low-signal-intensity center (arrowhead). **(c)** Contrast-enhanced sagittal T1-weighted MR image demonstrates the mildly enhancing oval intramedullary mass (arrows) at C2. **(d)** Axial T1-weighted MR image obtained at the level of the tumor shows the intramedullary lesion (arrows) with expansion of the cord. *v* = vertebral body.

ous nonneoplastic causes of intramedullary expansion reported in the literature: epidermoid cyst associated with an extraspinal (mediastinal) neurenteric cyst (123), congenital lipoma (124, 125), pseudocyst following prior spinal trauma (126), Wegener granuloma (4), cavernous malformations (127), and abscess (128).

Summary

As a group, intramedullary spinal neoplasms have limited distinguishing features on radiologic images. In adults, ependymomas are the most common intramedullary spinal neoplasms; astrocytomas are the second most common. In children, the relationship is reversed. Although there are no pathognomonic imaging findings that allow flawless differentiation of an ependymoma from an astrocytoma in all cases, the combination of MR imaging findings often permits one most likely diagnosis to be posited. Features that favor an ependymoma include a central location; a well-circumscribed mass; the presence of hemorrhage; a location in the conus medullaris or filum terminale; and focal, intense, homogeneous enhancement. Astrocytoma is favored when the mass is eccentric, is ill-defined, and enhances in a patchy, irregular fashion. Myxopapillary ependymoma is the most common neoplasm of the conus medullaris or filum terminale. Gangliogliomas characteristically involve eight or more vertebral segments and have mixed signal intensity on T1-weighted images, a finding unique among spinal cord tumors. Hemangioblastomas and paragangliomas, which are both highly vascular lesions, may have prominent flow voids near the mass and may manifest with the cap sign, which is classically associated with ependymomas. Less common intraspinal neoplasms include metastases, lymphoma, and PNET.

Acknowledgments: The authors gratefully acknowledge the contributions of case material to the Thompson Archives of the Department of Radiologic Pathology from radiology residents worldwide and editorial assistance from Melissa L. Rosado de Christenson, Col, USAF, MC, of the AFIP and John L. D. Atkinson, MD, of the Mayo Clinic, Rochester, Minn.

References

1. Constantini S, Houten J, Miller D, et al. Intramedullary spinal cord tumors in children under the age of 3 years. J Neurosurg 1996; 85: 1036–1043.
2. Sze G, Stimac GK, Bartlett C, et al. Multicenter study of gadopentetate dimeglumine as an MR contrast agent: evaluation in patients with spinal tumors. AJNR Am J Neuroradiol 1990; 11:967–974.
3. Georgy BA, Hesselink JR. MR imaging of the spine: recent advances in pulse sequences and special techniques. AJR Am J Roentgenol 1994; 162:923–934.
4. Valk J. Gd-DTPA in MR of spinal lesions. AJNR Am J Neuroradiol 1988; 9:345–350.
5. Epstein FJ, Farmer JP, Freed D. Adult intramedullary spinal cord ependymomas: the result of surgery in 38 patients. J Neurosurg 1993; 79: 204–209.
6. Parizel PM, Balériaux D, Rodesch G, et al. Gd-DTPA–enhanced MR imaging of spinal tumors. AJR Am J Roentgenol 1989; 152:1087–1096.
7. Epstein FJ, Farmer JP, Freed D. Adult intramedullary astrocytomas of the spinal cord. J Neurosurg 1992; 77:355–359.
8. Brotchi J, Dewitte O, Levivier M, et al. A survey of 65 tumors within the spinal cord: surgical results and the importance of preoperative magnetic resonance imaging. Neurosurgery 1991; 29: 651–657.
9. Takemoto K, Matsumura Y, Hashimoto H, et al. MR imaging of intraspinal tumors: capability in histological differentiation and compartmentalization of extramedullary tumors. Neuroradiology 1988; 30:303–309.
10. Lee M, Epstein FJ, Rezai AR, Zagzag D. Nonneoplastic intramedullary spinal cord lesions mimicking tumors. Neurosurgery 1998; 43:788–795.
11. Andrews BT, Weinstein PR, Rosenblum ML, Barbaro NM. Intradural arachnoid cysts of the spinal canal associated with intramedullary cysts. J Neurosurg 1988; 68:544–549.
12. Dillon WP, Norman D, Newton TH, Bolla K, Mark AS. Intradural spinal cord lesions: Gd-DTPA–enhanced MR imaging. Radiology 1989; 170:229–237.
13. Sze G, Krol G, Zimmerman RD, Deck MDF. Intramedullary disease of the spine: diagnosis using gadolinium-DTPA–enhanced MR imaging. AJR Am J Roentgenol 1988; 151:1193–1204.
14. Goy AMC, Pinto RS, Raghavendra BN, Epstein FJ, Kricheff II. Intramedullary spinal cord tumors: MR imaging, with emphasis on associated cysts. Radiology 1986; 161:381–386.
15. Bydder GM, Brown J, Niendorf HP, Young IR. Enhancement of cervical intraspinal tumors in MR imaging with intravenous gadolinium-DTPA. J Comput Assist Tomogr 1985; 9:847–851.
16. Froment JC, Balériaux D, Turjman F, Patay Z, Rio F. Diagnosis: neuroradiology. In: Fischer G, Brotchi J, eds. Intramedullary spinal cord tumors. Stuttgart, Germany: Thieme, 1996; 33–52.
17. Epstein FJ, Farmer JP, Schneider SJ. Intraoperative ultrasonography: an important surgical adjunct for intramedullary tumors. J Neurosurg 1991; 74:729–733.
18. Epstein F, Epstein N. Surgical treatment of spinal cord astrocytomas of childhood. J Neurosurg 1982; 57:685–689.
19. Ferrante L, Mastronardi L, Celli P, Lunardi P, Acqui M, Fortuna A. Intramedullary spinal cord ependymomas: a study of 45 cases with long-term follow-up. Acta Neurochir 1992; 119:74–79.
20. Lee M, Rezai AR, Freed D, Epstein FJ. Intramedullary spinal cord tumors in neurofibromatosis. Neurosurgery 1996; 38:32–37.
21. Epstein F, Wisoff J. Intra-axial tumors of the cervicomedullary junction. J Neurosurg 1987; 67:483–487.
22. Robertson PL, Allen JC, Abbott IR, Miller DC, Fidel J, Epstein FJ. Cervicomedullary tumors in children: a distinct subset of brainstem gliomas. Neurology 1994; 44:1798–1803.
23. Samii M, Klekamp J. Surgical results of 100 intramedullary tumors in relation to accompanying syringomyelia. Neurosurgery 1994; 35:865–873.
24. Brotchi J, Fischer G. Treatment. In: Fischer G, Brotchi J, eds. Intramedullary spinal cord tumors. Stuttgart, Germany: Thieme, 1996; 60–84.
25. Hoshimaru M, Koyama T, Hashimoto N, Kikuchi H. Results of microsurgical treatment for intramedullary spinal cord ependymomas: analysis of 36 cases. Neurosurgery 1999; 44:264–269.
26. Helwig EB, Stern JB. Subcutaneous sacrococcygeal myxopapillary ependymoma: a clinicopathologic study of 32 cases. Am J Clin Pathol 1984; 81:156–161.
27. Morantz RA, Kepes JJ, Batinsky S, Masterson BJ. Extraspinal ependymomas: report of three cases. J Neurosurg 1979; 51:383–391.
28. Hawkins CP, Heron JR. Subarachnoid hemorrhage from spinal tumor (letter). J Neurol Neurosurg Psychiatry 1988; 51:305–307.
29. Djindjian M, Djindjian R, Houdart R, Hurth M. Subarachnoid hemorrhage due to intraspinal tumors. Surg Neurol 1978; 9:223–229.
30. Cooper P. Outcome after operative treatment of intramedullary spinal cord tumors in adults: intermediate and long-term results in 51 patients. Neurosurgery 1989; 25:855–859.
31. Wolff M, Santiago H, Duby MM. Delayed distant metastasis from a subcutaneous sacrococcygeal ependymoma: case report with tissue culture, ultrastructural observations, and review of the literature. Cancer 1972; 30:1046–1067.

32. Burger PC, Scheithauer BW. Tumors of neuroglia and choroid plexus epithelium. In: Burger PC, Scheithauer BW, eds. Tumors of the central nervous system. Washington, DC: Armed Forces Institute of Pathology, 1994; 25–161.
33. Moser FG, Tuvia J, LaSalla P, Llana J. Ependymoma of the spinal nerve root: case report. Neurosurgery 1992; 31:962–964.
34. Birch BD, Johnson JP, Parsa A, et al. Frequent type 2 neurofibromatosis gene transcript mutations in sporadic intramedullary spinal cord ependymomas. Neurosurgery 1996; 39:135–140.
35. Fine MJ, Kricheff II, Freed D, Epstein FJ. Spinal cord ependymomas: MR imaging features. Radiology 1995; 197:655–658.
36. Kahan H, Sklar EML, Post MJD, Bruce JH. MR characteristics of histopathologic subtypes of spinal ependymoma. AJNR Am J Neuroradiol 1996; 17:143–150.
37. Lohle PN, Wurzer HA, Hoogland PH, Seelen PJ, Go KG. The pathogenesis of syringohydromyelia in spinal cord ependymoma. Clin Neurol Neurosurg 1994; 96:323–326.
38. Wiestler OD, Schiffer D, Coons SW, Prayson RA, Rosenblum MK. Myxopapillary ependymoma. In: Kleihues P, Cavenee WK, eds. Pathology and genetics of tumours of the central nervous system. 3rd ed. Lyon, France: International Agency for Research on Cancer, 2000.
39. Wippold FJ II, Smirniotopoulos JG, Moran CJ, Suojanen JN, Vollmer DG. MR imaging of myxopapillary ependymoma: findings and value to determine extent of tumor and its relations to intraspinal structures. AJR Am J Roentgenol 1995; 165:1263–1267.
40. Moelleken SMC, Seeger LL, Eckhardt JJ, Batzdorf U. Myxopapillary ependymoma with extensive sacral destruction: CT and MR findings. J Comput Assist Tomogr 1992; 16:164–166.
41. Osborn AG. Tumors, cysts, and tumorlike lesions of the spine and spinal cord. In: Osborn A, ed. Diagnostic neuroradiology. St Louis, Mo: Mosby–Year Book, 1994; 895–916.
42. Wippold FJ II, Smirniotopoulos JG. Presence of superficial siderosis assists in the diagnosis of myxopapillary ependymoma (letter). AJR Am J Roentgenol 1996; 166:1493–1494.
43. Scheithauer BW. Symptomatic subependymoma: report of 21 cases with review of the literature. J Neurosurg 1978; 49:689–696.
44. Jallo GI, Zagzag D, Epstein F. Intramedullary subependymoma of the spinal cord. Neurosurgery 1996; 38:251–257.
45. Artico M, Bardella L, Ciappetta P, Raco A. Surgical treatment of subependymomas of the central nervous system: report of 8 cases and review of the literature. Acta Neurochirugica 1989; 98: 25–31.
46. Hoeffel C, Boukobza M, Polivka M, et al. MR manifestations of subependymomas. AJNR Am J Neuroradiol 1995; 16:2121–2129.
47. Cohen AR, Wisoff JH, Allen JC, Epstein F. Malignant astrocytomas of the spinal cord. J Neurosurg 1989; 70:50–54.
48. Bell WO, Packer RJ, Seigel KR, et al. Leptomeningeal spread of intramedullary spinal cord tumors. J Neurosurg 1988; 69:295–300.
49. Lindstadt DE, Wara WM, Leibel SA, Gutin PH, Wilson CB, Sheline GE. Postoperative radiotherapy of primary spinal cord tumors. Int J Radiat Oncol Biol Phys 1989; 16:1397–1403.
50. Ciappetta P, Salvati M, Capoccia G, et al. Spinal glioblastomas: report of seven cases and review of the literature. Neurosurgery 1991; 28:302–306.
51. Hamburger C, Buttner A, Weis S. Ganglioglioma of the spinal cord: report of two rare cases and review of the literature. Neurosurgery 1997; 41: 1410–1416.
52. Patel U, Pinto RS, Miller DC, et al. MR of spinal cord ganglioglioma. AJNR Am J Neuroradiol 1998; 19:879–887.
53. Furie DM, Felsberg G, Tien RD, Friedman HS, Fuchs H, McLendon R. MRI of gangliocytoma of cerebellum and spinal cord. J Comput Assist Tomogr 1993; 17:488–491.
54. Nakajima M, Kidooka M, Nakasu S. Anaplastic ganglioglioma with dissemination to the spinal cord: a case report. Surg Neurol 1998; 49:445–448.
55. Wald U, Levy PJ, Rappaport ZH, Michowitz SD, Schuger L, Shalit MN. Conus ganglioglioma in a 2 1/2-year-old boy: case report. J Neurosurg 1985; 62:142–144.
56. Quinn B. Synaptophysin staining for gangliogliomas (letter). AJNR Am J Neuroradiol 1999; 20:526–529.
57. Murota T, Symon L. Surgical management of hemangioblastoma of the spinal cord: a report of 18 cases. Neurosurgery 1989; 25:699–708.
58. Xu QW, Bao WM, Mao RL, Yang GY. Magnetic resonance imaging and microsurgical treatment of intramedullary hemangioblastomas of the spinal cord. Neurosurgery 1994; 35:671–676.
59. Arbelaez A, Castillo M, Armao D. Hemangioblastoma of the filum terminale. AJR Am J Roentgenol 1999; 173:857–858.
60. Neumann HPH, Eggert HR, Weigel K, Friedburg H, Wiestler OD, Schollmeyer P. Hemangioblastomas of the central nervous system: a 10-year study with special reference to von Hippel–Lindau syndrome. J Neurosurg 1989; 70:24–30.
61. Browne TR, Adams RD, Robertson GH. Hemangioblastoma of the spinal cord. Arch Neurol 1976; 33:435–441.
62. Sze G. Neoplastic disease of the spine and spinal cord. In: Atlas S, ed. Magnetic resonance imaging of the brain and spine. 2nd ed. Philadelphia, Pa: Lippincott-Raven, 1996; 1370–1380.
63. Cerejo A, Vaz R, Feyo PB, Cruz C. Spinal cord hemangioblastoma with subarachnoid hemorrhage. Neurosurgery 1990; 27:991–993.
64. Rothstein T. Paraplegia resulting from rupture of previously asymptomatic intramedullary hemangioblastoma during coitus (letter). Ann Neurol 1985; 17:519.
65. Kormos RL, Tucker WS, Bilbao JM, Gladstone RM, Bass AG. Subarachnoid hemorrhage due to a spinal cord hemangioblastoma: case report. Neurosurgery 1980; 6:657–660.
66. Yu JS, Short MP, Schumacher J, Chapman PH, Harsh GR IV. Intramedullary hemorrhage in spinal cord hemangioblastoma: report of two cases. J Neurosurg 1994; 81:937–940.

67. Burger PC, Scheithauer BW. Tumors of uncertain origin. In: Burger PC, Scheithauer BW, eds. Tumors of the central nervous system. Washington, DC: Armed Forces Institute of Pathology, 1994; 239–249.
68. Corr P, Dicker T, Wright M. Exophytic intramedullary hemangioblastoma presenting as an extramedullary mass on myelography. AJNR Am J Neuroradiol 1995; 16:883–884.
69. Baker KB, Moran CJ, Wippold FJ II, et al. MR imaging of spinal hemangioblastomas. AJR Am J Roentgenol 2000; 174:377–382.
70. Kaffenberger DA, Shah CP, Murtagh FR, Wilson C, Silbiger ML. MR imaging of spinal cord hemangioblastoma associated with syringomyelia. J Comput Assist Tomogr 1988; 12:495–498.
71. Seeger JF, Burke DP, Knake JE, Gabrielsen TO. Computed tomographic and angiographic evaluation of hemangioblastomas. Radiology 1981; 138: 65–73.
72. Balériaux D, Parizel P, Bank WO. Intraspinal and intramedullary pathology. In: Manelfe C, ed. Imaging of the spine and spinal cord. New York, NY: Raven, 1992; 514–523.
73. Silbergeld J, Cohen WA, Maravilla K, Dalley RW, Sumi M. Supratentorial and spinal cord hemangioblastomas: gadolinium-enhanced MR appearance with pathologic correlation. J Comput Assist Tomogr 1989; 13:1048–1051.
74. Mascalchi M, Quilici N, Ferrito G, et al. Identification of the feeding arteries of spinal vascular lesions via phase-contrast MR angiography with three-dimensional acquisition and phase display. AJNR Am J Neuroradiol 1997; 18:351–358.
75. Rao AB, Koeller KK, Adair CF. Paragangliomas of the head and neck: radiologic-pathologic correlation. RadioGraphics 1999; 19:1605–1632.
76. Lerman RI, Kaplan ES, Daman L. Ganglioneuroma-paraganglioma of the intradural filum terminale. J Neurosurg 1972; 36:652–658.
77. Moran CA, Rush W, Mena H. Primary spinal paragangliomas: a clinicopathological and immunohistochemical study of 30 cases. Histopathology 1997; 31:167–171.
78. Sonneland PRL, Scheithauer BW, Lechago J, Crawford BG, Onofrio BM. Paraganglioma of the cauda equina region: clinicopathologic study of 31 cases with special reference to immunocytology and ultrastructure. Cancer 1986; 58:1720–1735.
79. Boker DK, Wassmann H, Solymosi L. Paragangliomas of the spinal canal. Surg Neurol 1983; 19:461–468.
80. Sharma A, Gaikwad SB, Goyal M, Mishra NK, Sharma MC. Calcified filum terminale paraganglioma causing superficial siderosis. AJR Am J Roentgenol 1998; 170:1650–1652.
81. Mammourian AC. MR of superficial siderosis (letter). AJNR Am J Neuroradiol 1993; 14:1445–1448.
82. Burger PC, Scheithauer BW. Tumors of paraganglionic tissue. In: Burger PC, Schetihauer BW, eds. Tumors of the central nervous system. Washington, DC: Armed Forces Institute of Pathology, 1994; 317–320.
83. Lack EE. Tumors of the adrenal gland and extraadrenal paraganglia. In: Rosai J, ed. Atlas of tumor pathology. Vol 19. Washington, DC: Armed Forces Institute of Pathology, 1997; 303–409.
84. Yoshida A, Umekita Y, Ohi Y, Hatanaka S, Yoshida H. Paraganglioma of the cauda equina: a case report and review of the literature. Acta Pathol Jpn 1991; 41:305–310.
85. Solymosi L, Ferbert A. A case of spinal paraganglioma. Neuroradiology 1985; 27:217–219.
86. Iliya AR, Davis RP, Seidman RJ. Paraganglioma of the cauda equina: case report with magnetic resonance imaging description. Surg Neurol 1991; 35:366–367.
87. Aggarwal S, Deck JHN, Kucharczyk W. Neuroendocrine tumor (paraganglioma) of the cauda equina: MR and pathological findings. AJNR Am J Neuroradiol 1993; 14:1003–1007.
88. Hayes E, Lippa C, Davidson R. Paragangliomas of the cauda equina. AJNR Am J Neuroradiol 1989; 10(suppl):S45–S47.
89. Faro SH, Turtz AR, Koenigsberg RA, Mohamed FB, Chen CY, Stein H. Paraganglioma of the cauda equina with associated intramedullary cyst: MR findings. AJNR Am J Neuroradiol 1997; 18: 1588–1590.
90. Steel TR, Botterill P, Sheehy JP. Paraganglioma of the cauda equina with associated syringomyelia: case report. Surg Neurol 1994; 42:489–493.
91. Costigan DA, Winkelman MD. Intramedullary spinal cord metastasis: a clinicopathological study of 13 cases. J Neurosurg 1985; 62:227–233.
92. Findlay JM, Bernstein M, Vanderlinden RG, Resch L. Microsurgical resection of solitary intramedullary spinal cord metastases. Neurosurgery 1987; 21:911–915.
93. Sevick RJ. Cervical spine tumors. In: Ross J, ed. The cervical spine. Philadelphia, Pa: Saunders, 1995; 385–400.
94. Zumpano BJ. Spinal intramedullary metastatic medulloblastoma. J Neurosurg 1978; 48:632–635.
95. Barnwell SL, Edwards MSB. Spinal intramedullary spread of medulloblastoma. J Neurosurg 1986; 65:253–255.
96. Lim V, Sobel DF, Zyroff J. Spinal cord pial metastases: MR imaging with gadopentetate dimeglumine. AJNR Am J Neuroradiol 1990; 11:975–982.
97. Post MJD, Quencer RM, Green BA, et al. Intramedullary spinal cord metastasis, mainly of nonneurogenic origin. AJNR Am J Neuroradiol 1987; 8:339–346.
98. Koeller KK, Smirniotopoulos JG, Jones RV. Primary central nervous system lymphoma: radiologic-pathologic correlation. RadioGraphics 1997; 17:1497–1526.
99. Schild SE, Wharen RE Jr, Menke DM, Folger WN, Colon-Otero G. Primary lymphoma of the spinal cord. Mayo Clin Proc 1995; 70:256–260.

100. Urasaki E, Yamada H, Tokimura T, Yokota A. T-cell type primary spinal intramedullary lymphoma associated with human T-cell lymphotropic virus type I after a renal transplant: case report. Neurosurgery 1996; 38:1036–1039.
101. Bluemke DA, Wang H. Primary spinal cord lymphoma: MR appearance. J Comput Assist Tomogr 1990; 14:812–814.
102. Caruso PA, Patel MR, Joseph J, Rachlin J. Primary intramedullary lymphoma of the spinal cord mimicking cervical spondylitic myelopathy. AJR Am J Roentgenol 1998; 171:526–527.
103. Henry JM, Heffner RR, Dillard SH, Earle KM, Davis RL. Primary malignant lymphomas of the central nervous system. Cancer 1974; 34:1293–1302.
104. O'Neill BP, Illig JJ. Primary central nervous system lymphoma. Mayo Clin Proc 1989; 64:1005–1020.
105. Herbst K, Corder M, Justice G. Successful therapy with methotrexate of a multicentric mixed lymphoma of the central nervous system. Cancer 1976; 38:1476–1478.
106. Itami J, Mori S, Arimizu N, Inoue S, Lee M, Uno K. Primary intramedullary spinal cord lymphoma: report of a case. Jpn J Clin Oncol 1986; 16:407–412.
107. Deme S, Ang LC, Skaf G, Rowed D. Primary intramedullary primitive neuroectodermal tumor of the spinal cord: case report and review of the literature. Neurosurgery 1997; 41:1417–1420.
108. Kwon OK, Wang KC, Kim CJ, Kim IO, Chi JG, Cho BK. Primary intramedullary spinal cord primitive neuroectodermal tumor with intracranial seeding in an infant. Childs Nerv Syst 1996; 12:633–636.
109. Cidis-Meltzer C, Townsend D, Kottapally S, Jadali F. FDG imaging of spinal cord primitive neuroectodermal tumor. J Nucl Med 1998; 39: 1207–1209.
110. Papadatos D, Albrecht S, Mohr G, del Carpio-O'Donovan R. Exophytic primitive neuroectodermal tumor of the spinal cord. AJNR Am J Neuroradiol 1998; 19:787–789.
111. Prados MD, Edwards MSB, Chang SM, et al. Hyperfractionated craniospinal radiation therapy for primitive neuroectodermal tumors: results of a phase II study. Int J Radiat Oncol Biol Phys 1999; 43:279–285.
112. Koot RW, Henneveld HT, Albrecht KW. Two children with unusual causes of torticollis: primitive neuroectodermal tumor and Grisel's syndrome. Ned Tijdschr Geneeskd 1998; 142:1030–1033. [Dutch]
113. Covelli EM, Stefano ML, Panico L, Elmo M, Frezza P, Brunetti A. Primary neuroectodermal tumor with unusual spinal cord localization: a case report. Radiol Med (Torino) 1995; 89:362–364. [Italian]
114. Sevick RJ, Johns RD, Curry BJ. Primary spinal primitive neuroectodermal tumor with extraneural metastases. AJNR Am J Neuroradiol 1987; 8: 1151–1152.
115. Ogasawara H, Kiya K, Muttaqin KK, et al. Intracranial metastasis from a spinal cord primitive neuroectodermal tumor: case report. Surg Neurol 1992; 37:307–312.
116. Hart MN, Earle KM. Primitive neuroectodermal tumors of the brain in children. Cancer 1973; 32: 890–897.
117. Burger PC, Scheithauer BW. Embryonal tumors. In: Burger PC, Scheithauer BW, eds. Tumors of the central nervous system. Washington, DC: Armed Forces Institute of Pathology, 1994; 193–225.
118. Becker LE, Hinton D. Primitive neuroectodermal tumors of the central nervous system. Hum Pathol 1983; 14:538–550.
119. Rorke LB. The cerebellar medulloblastoma and its relationship to primitive neuroectodermal tumors. J Neuropath Exp Neurol 1983; 42:1–15.
120. Freyer DR, Hutchinson RJ, McKeever PE. Primary primitive neuroectodermal tumor of the spinal cord associated with neural tube defect. Pediatr Neurosci 1989; 15:181–187.
121. Salvati M, Artico M, Lunardi P, Gagliardi FM. Intramedullary meningioma: case report and review of the literature. Surg Neurol 1992; 37:42–45.
122. Gorman P, Rigamonti D, Joslyn JN. Intramedullary and extramedullary schwannoma of the cervical spinal cord: case report. Surg Neurol 1989; 32:459–462.
123. Tekkok IH, Palasoglu S, Erbengi A, Onol B. Intramedullary epidermoid cyst of the cervical spinal cord associated with an extraspinal neurenteric cyst: case report. Neurosurgery 1992; 31: 121–125.
124. Ur-Rahman N, Salih MAM, Jamjoom AH, Jamjoom ZA. Congenital intramedullary lipoma of the dorsocervical spinal cord with intracranial extension: case report. Neurosurgery 1994; 34: 1081–1084.
125. Aoki N. Syringomyelia secondary to congenital intraspinal lipoma. Surg Neurol 1991; 35:360–365.
126. Chuang KS, Wang YC, Tsai SH, Liu MY. Spinal intramedullary pseudocyst. J Neurosurg 1985; 63:453–455.
127. Anson JA, Spetzler RF. Surgical resection of intramedullary spinal cord cavernous malformations. J Neurosurg 1993; 78:446–451.
128. Blacklock JB, Hood TW, Maxwell RE. Intramedullary cervical spinal cord abscess. J Neurosurg 1982; 57:270–273.

This article meets the criteria for 1.0 credit hour in category 1 of the AMA Physician's Recognition Award. To obtain credit, see accompanying test at http://www.rsna.org/education/rg_cme.html.